CaO-β QUARTZ REACTION AT MODERATE TEMPERATURES

CaO-β QUARTZ REACTION AT MODERATE TEMPERATURES

by

ARVIND S. BURTE

A Thesis

Submitted to the School of Graduate Studies

in Partial Fulfilment of the Requirements

for the Degree

Master of Engineering

McMaster University

October, 1971

MASTER OF ENGINEERING
(Metallurgy and Materials Science)

McMASTER UNIVERSITY
Hamilton, Ontario

TITLE: CaO-β Quartz Reaction at Moderate Temperatures

AUTHOR: Arvind S. Burte, B.Tech. (Indian Institute of Technology)

SUPERVISOR: Dr. P. S. Nicholson

NUMBER OF PAGES: (viii), 86.

SCOPE AND CONTENTS:

An investigation is reported on the kinetics of CaO-β quartz solid state reaction on basal and prism planes of β-quartz at temperatures in the range between $1000^{\circ}C$ and $1200^{\circ}C$. Excess lime present in all the samples ensured the formation of C_2S (dicalcium silicate) only. The thickness of the C_2S product layer was measured on a Zeiss camera microscope Ultraphot II. The line scans for the distribution of Ca and Si across the reaction layer were obtained on the electron microprobe analyser. The kinetics of the reaction on basal and prism planes of β-quartz in wet and dry nitrogen atmospheres in the temperature range considered was studied by measuring the thickness of C_2S as a function of time of reaction.

The CaO-β quartz reaction was found to be anisotropic, the basal plane reaction being faster than the prism plane reaction. The reaction on both basal and prism planes in the temperature range between $1000^{\circ}C$ and $1200^{\circ}C$ was found to be enhanced in the presence of moisture. The enhancement due to the presence of moisture was found to be more on the basal plane reaction than on the prism plane reaction. This appears to be due to the fact that different

polymorphs of C_2S with different sensitivities to the presence of moisture are produced on different crystallographic planes of β-quartz considered. The activation energies for the reaction on basal plane and prism plane were found to be about 53 kcal/mole and 63 kcal/mole respectively. They have good agreement with the activation energies of 55 kcal/mole and 65 kcal/mole for Ca diffusion in α-C_2S and α'-C_2S respectively as reported by Lindner.

ACKNOWLEDGMENTS

TABLE OF CONTENTS

LIST OF FIGURES

(vii)

LIST OF TABLES

CHAPTER 1

INTRODUCTION AND LITERATURE SURVEY

A. Introduction

The reaction between CaO and SiO_2 in solid state at high temperatures has been extensively explored owing to its commercial importance. Calcium silicates are the compounds chiefly responsible for the setting and hardening actions on mixing cement with water.

Raw portland cement is a mixture of lime (CaO) and silica (SiO_2), alumina (Al_2O_3) and iron (Fe_2O_3) and a small percentage of sulphur trioxide (SO_3) which is added subsequent to calcination to retard the set of the finished product. Proper combination of these oxides when heated to incipient fusion at optimum burning temperatures in a cement kiln can be assured by close control of the ratios of the various oxides involved[1]. When such control measures are not applied "overliming" may result with the consequent presence of uncombined lime in the finished product. Uncombined or free lime in sufficient quantities causes the cement to be unsound, i.e., produces excessive expansion of the hardened cement paste. "Underliming" may result from improper mix control and is undesirable since the resulting product has low-strength properties.

When cement raw materials containing proper proportions of the essential oxides are ground to a suitable fineness and then burned to

incipient fusion in a cement kiln, chemical combination takes place largely
in the solid state resulting in a product termed "clinker". The cumulative
efforts of such investigators as Rankin and Wright[2], Swayze[3] and others
towards finding the constitution of portland cement clinker have indicated
that the essential compounds are silicates of lime, i.e., tricalcium silicate
(3 CaO . SiO_2 or C_3S) and dicalcium silicate (2 CaO . SiO_2 or C_2S). Signifi-
cant amounts of tricalcium aluminate are also present. When magnesia is
present as it usually is, there appears to be no combination between it and
other oxides. Magnesia crystallises out of solid solution on slow cooling
to form interstitial magnesia crystals which have been found to react very
slowly with water and thus cause detrimental delayed expansion of concrete.
If, on the other hand, portland cement clinker is quick quenched at a suit-
able temperature, the magnesia is frozen in solid solution and the subsequent
detrimental expansion in concrete may be eliminated. The calcareous materials
used for making portland cement are limestone, marl, cement rock and marine
shells and the argillaceous materials are clay, shale, slate, blast furnace
slag and ashes[4].

There is no stage in the manufacture of portland cement that equals
in importance the conversion of the proper chemically designed and physically
prepared raw material into clinker through the controlled combustion of solid,
liquid or gaseous fuels in a rotary kiln and the subsequent proper quenching
and cooling of the clinker. From the invention of portland cement in 1824
until 1866, clinker was made by a batch process in vertical kilns. Then
the rotary kiln came into use. Decreasing the amount of fuel required for

the production of clinker has been the most important goal in the development of rotary kilns. Typical analyses of some portland cements are shown in Table I.1[5].

If the clinkering operation is to be performed at low temperatures, the quality of the clinker might be affected because of the poor reaction kinetics at low temperatures. Typical clinkering temperatures are $1400^{o}C$ or $1500^{o}C$. The feasibility of carrying out the clinkering at low temperatures like $1200^{o}C$ or $1100^{o}C$ has to be decided by the kinetic study of CaO-SiO_2 reaction and ways of improving kinetics have to be investigated. This has been the aim in many of the studies of the CaO-SiO_2 solid state reaction.

Compounds of silica and calcia are also important in ceramic technology. Wollastonite[6] (theoretical composition SiO_2 51.75%, CaO 48.25%) has a high fluxing action and brings down the maturing point of ceramic bodies when developed in the ware. Wollastonite does not evolve a gas on heating. Hence it can be successfully used in the low temperature glost firing of bisque ceramic ware with no carbonate-associated defect generation. Hence its incorporation in wall tiles can replace a double firing by single firing schedule. Wollastonite bodies have good resistance to thermal shock. Wollastonite is also used in low-loss electrical bodies fired at lower temperatures.

Calcium oxide and silica are constituents of many refractories. Table I.2 shows compositions of some such refractories. The most common domestic and commercial glasses incorporate lime and silica in their compositions. Some typical soda-lime-silica glass mixes are shown in Table I.3.

TABLE I.1

TYPICAL ANALYSES OF SOME PORTLAND CEMENTS

	Type 1	Type 2	Type 3	Type 4	Type 5
Silicon dioxide (SiO_2), min, %		21.0			
Aluminum oxide (Al_2O_3), max, %		6.0			
Ferric oxide (Fe_2O_3), max, %		6.0		6.5	
Magnesium oxide (MgO), max, %	5.0	5.0	5.0	5.0	4.0
Sulfur trioxide (SO_3), max, %:					
when $3CaO.Al_2O_3$ is 8% or less	2.5	2.5	3.0	2.3	2.3
when $3CaO.Al_2O_3$ is more than 8%	3.0		4.0		
Loss on ignition, max, %	3.0	3.0	3.0	2.5	3.0
Insoluble residue, max, %	0.75	0.75	0.75	0.75	0.75
Tricalcium silicate ($3CaO.SiO_2$), max, %				35	
Dicalcium silicate ($2CaO.SiO_2$), max, %				40	
Tricalcium aluminate ($3CaO.Al_2O_3$), max, %		8	15	7	5
Sum of tricalcium silicate and tricalcium aluminate, max, %		58			
Tetracalcium aluminoferrite plus twice the tricalcium aluminate ($4CaO.Al_2O_3.Fe_2O_3 + 2(3CaO.Al_2O_3)$), or solid solution ($4CaO.Al_2O_3.Fe_2O_3 + 2CaO.Fe_2O_3$), as applicable, max, %					20

TABLE I.2

COMPOSITIONS OF SOME REFRACTORIES CONTAINING LIME AND SILICA

Body Type	Composition	
Magnesite refractory	MgO	80 - 90%
	CaO	3 - 12%
	SiO_2	$\approx$ 3%
	Fe_2O_3	1 - 2%
	Al_2O_3	1 - 4%
Periclase	MgO	95 - 99%
	CaO	0.2 - 2.6%
	SiO_2	0.1 - 1.9%
	Fe_2O_3	0 - 0.6%
	Al_2O_3	0 - 0.6%

TABLE I.3

COMPOSITIONS OF SOME TYPICAL SODA-LIME-SILICA GLASS MIXES

Glass Type	Composition	
Sheet	SiO_2	71 - 73%
	Na_2O	12 - 15%
	CaO	8 - 10%
	Al_2O_3	0.5 - 1.5%
Plate	SiO_2	71 - 73%
	Na_2O	12 - 14%
	CaO	10 - 12%
	Al_2O_3	0.5 - 1.5%
Lamp bulbs	SiO_2	73.6%
	Na_2O	16.0%
	H_2O	0.6%
	CaO	5.2%
	MgO	3.6%
	Al_2O_3	1.1%

B. Silica

The most important crystalline phases of silica[7] are:

(i)   Quartz: which is stable under atmospheric pressure from absolute
zero of temperature up to 867°C and is capable of metastable
existence at higher temperatures.

(ii)   Tridymite: which exists in two varieties, i.e., tridymite S,
stable under atmospheric pressure from 867°C to 1470°C and capable
of metastable existence both above 1470°C and below 867°C, and
tridymite M, metastable under atmospheric pressure at all tempera-
tures changing gradually into tridymite S at a rate which becomes
appreciable only above about 900°C.

(iii) Cristobalite: which is stable under atmospheric pressure from 1470°C
to 1723°C, its melting point, and capable of metastable existence
at any temperature below 1470°C.

Three other reported crystalline forms -- coesite, keatite and stishovite
are only producible at high pressures and are presumably basically stranded
under atmospheric pressure. The lightest known phase of silica is silica W,
which is formed by the oxidation of gaseous silicon monoxide (SiO).

The stable modification of silica under atmospheric pressure
from absolute zero to 573°C is low or α-quartz. At 573°C this changes
reversibly into high or β-quartz, which then remains stable up to 867°C.
Tridymite exhibits a complex series of high low inversion similar in part

to the 573°C inversion of quartz. Tridymite S has reversible inversions
at 64°, 117°, 163°, 210° and 415°C. Tridymite M, while changing slowly into
tridymite S, shows reversible high/low inversions at 117° and 163°C. The
cristobalite inversion is similar to that of quartz but is different in
that it occurs at a variable temperature depending upon the previous
history of the crystal and other factors.

Quantitative amounts of silica phases developed from pure quartz
by heating to 1500°C as a function of time are shown in Figure I.1.
The formation of cristobalite grains on the surface of a quartz grain
is shown in Figure I.2.

The low (α)-high (β) quartz inversion temperature under atmospheric
pressure is 573±1°C. The principal features of this inversion are:

(i) With rising temperature a general increase in the rate of change of
all physical properties of α-quartz occurs 50°C or so below the inversion
temperature,

(ii) The entire absence of such a preliminary effect with falling tempera-
ture on the β-quartz side of the inversion point,

(iii) A change of symmetry at the inversion point, and

(iv) An abrupt change in all the physical properties at the inversion
point.

The α-β quartz transformation involves a change in Si-O bond angles and
a volume expansion. No permanent change in any of the properties of pure
quartz has ever been observed as a result of its passage through the high-
low inversion and back again.
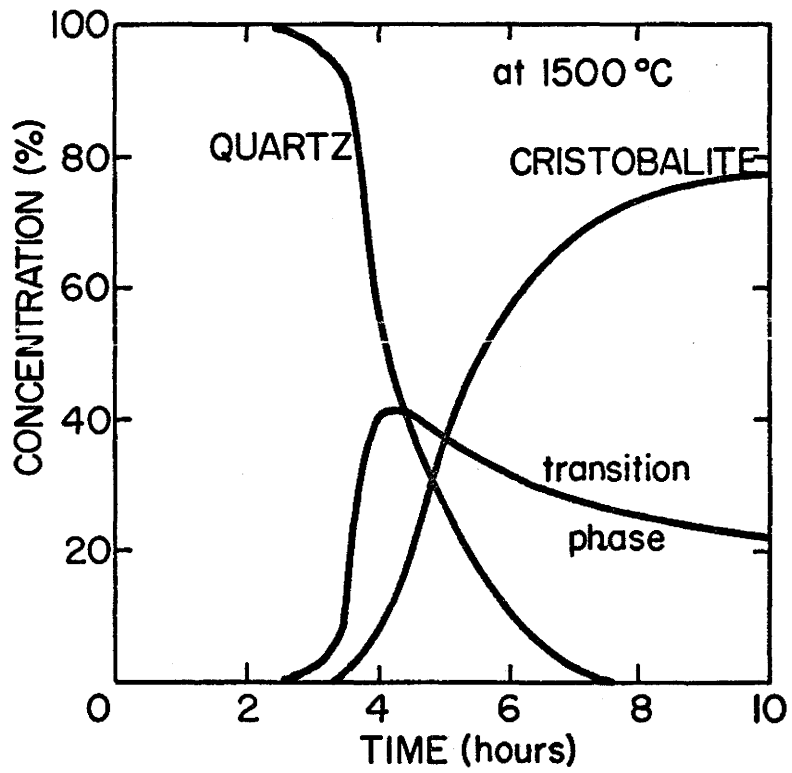
Figure I.1   Quantitative amounts of silica phases developed from pure quartz by heating to 1500°C, as a function of time.
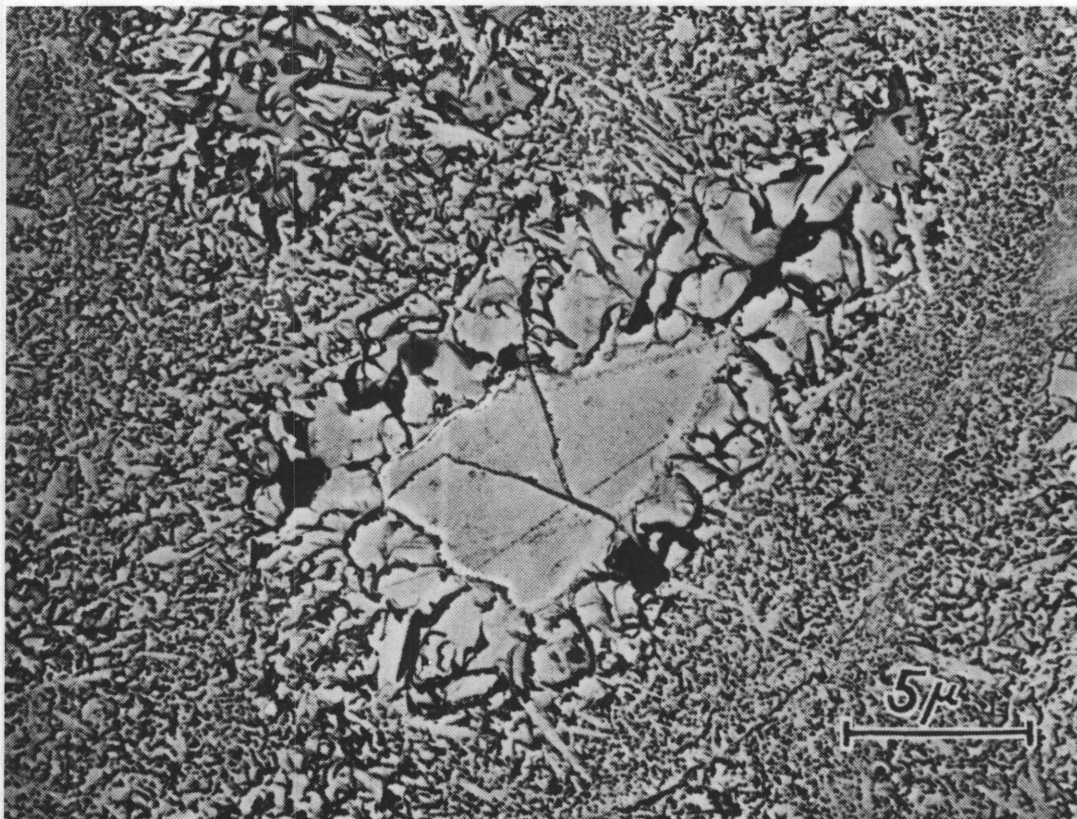
Figure I.2   Quartz grain with cristobalite formed at surface
(etched 20 min, 100°C, 50% NaOH, silica replica,
3650 X).

Many investigators have undertaken work on the effect of different variables such as impurities and particle size on the phase transformations of silica[8]. The direct conversion of quartz into tridymite by heat alone has not been definitely proved. It may sometimes occur, but it is certainly not the change which is usually observed[7]. For the conversion of quartz into tridymite the presence of a catalyst or a mineraliser is thought to be necessary. Keyser and Cypres[9] studied the formation of tridymite from pure quartz and the influence of CaO, Na_2O, Li_2O and K_2O thereon. They found that in the presence of CaO, the rate of transformation of quartz to tridymite is appreciable only after 1200^oC and reaches a peak between 1300^oC to 1350^oC.

Some of the naturally occurring forms of silica are:

(i)   Crystalline quartz,

(ii) Quartzite rock

(iii) Ganister

(iv) Sand and sandstone

(v)   Flint (a crystalline quartz held together by interstitial water)

In almost all the crystalline forms of silica and, in fact, in all silicates, the common molecular grouping is that of one silicon atom with four oxygen atoms for nearest neighbors and placed at the corners of a tetrahedron. The tetrahedron does not, however, have to be absolutely regular, i.e., possessed of four equal faces that are equilateral triangles.

Since the molecular composition of silica is SiO_2 and not SiO_4 elementary tetrahedra each containing a central silicon atom must share the oxygens such that an oxygen atom exists at each tetrahedral apex. The structures of silica differ only in the relative arrangement of the neighboring tetrahedra in space. In case of quartz, tridymite and cristo-

balite, the tetrahedra can be considered as joined corner to corner. The unit cell of both high and low quartz is hexagonal in the general sense and is shown in Figure I.3 . Table I.4 summarises the symmetry of the modifications of silica. The unit cell of high cristobalite (Figure I.4) is cubic with 8 silicon and 16 oxygen atoms.

Diffusion of Ca^{+2} or other cations in quartz is of fundamental importance in geological and ceramic studies. In his work on ionic diffusion and electrical conductivity in quartz, Verhoogen[10] found the following expressions for the diffusion coefficients of Li^+, Na^+, K^+ parallel to the c axis of natural quartz crystals in the range 300 to 500°C:

$$D_{Li} = 6.9 \times 10^{-3} \times e^{-20000/RT} \; cm^2/sec$$
$$D_{Na} = 3.6 \times 10^{-3} \times e^{-24000/RT} cm^2/sec$$
$$D_K = 0.18 \times e^{-31700/RT} \; cm^2/sec$$

In the same temperature range, the diffusion coefficients of Ca^{+2}, Mg^{+2}, Fe^{+2} are considerably smaller. It has been suggested here that electrical conduction parallel to the c axis of quartz results from motion of Frenkel oxygen defects. On this hypothesis, the coefficient of self diffusion of oxygen in quartz at 500°C was found to be approximately 3×10^{-11} cm^2/sec. That diffusion of alkali ions can take place perpendicular to the c axis also was demonstrated by Pfenninger and Laves[11]. Rybach and Laves[12] measured the diffusion of sodium into quartz under the driving force of a concentration gradient and found the relation $D = 3.8 \times 10^{-2} \exp(-24500/RT)$ describes the temperature dependence of the diffusion coefficient. White[13] diffused sodium and potassium ions from feldspar into quartz and other silicates. Hydrothermal solutions can also supply the necessary ions for diffusion. The activation energies are high but the piezoelectric voltages, although small,

Figure I.3   Schematic illustration of
relationship between:
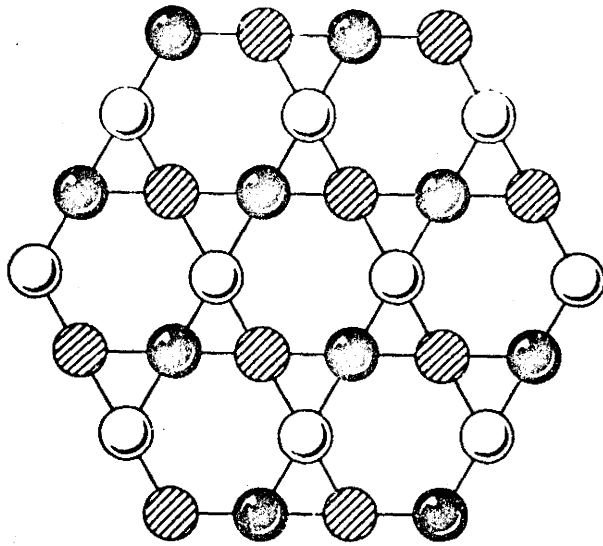
(a)
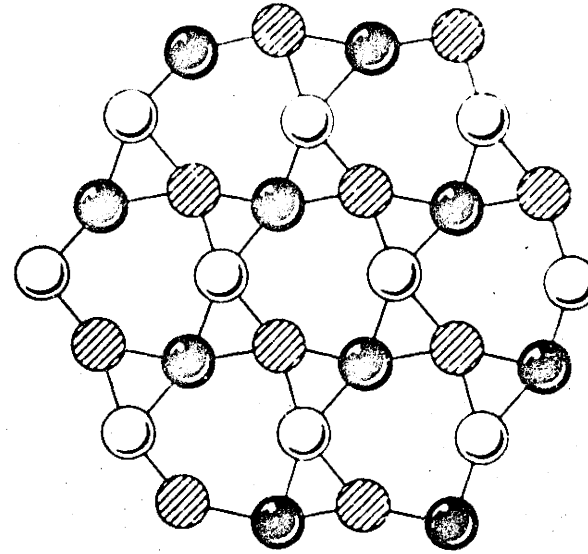
(b)

high temperature and   low temperature forms of quartz.

Circles indicate silicon centres only. Open circle indicates highest level,
hatched circle, intermediate level and black circle, lowest level.

TABLE I.4
SYMMETRY OF THE MODIFICATIONS OF SILICA

Modification of Silica	Symmetry of Unit Cell
Low quartz	Hexagonal
High quartz	Hexagonal
Tridymite S-I	Orthorhombic
Tridymite S-III	Hexagonal
Tridymite S-IV	Hexagonal
Low cristobalite	Tetragonal
High cristobalite	Isometric
Coesite	Monoclinic
Keatite	Tetragonal
Silica W	Orthorhombic
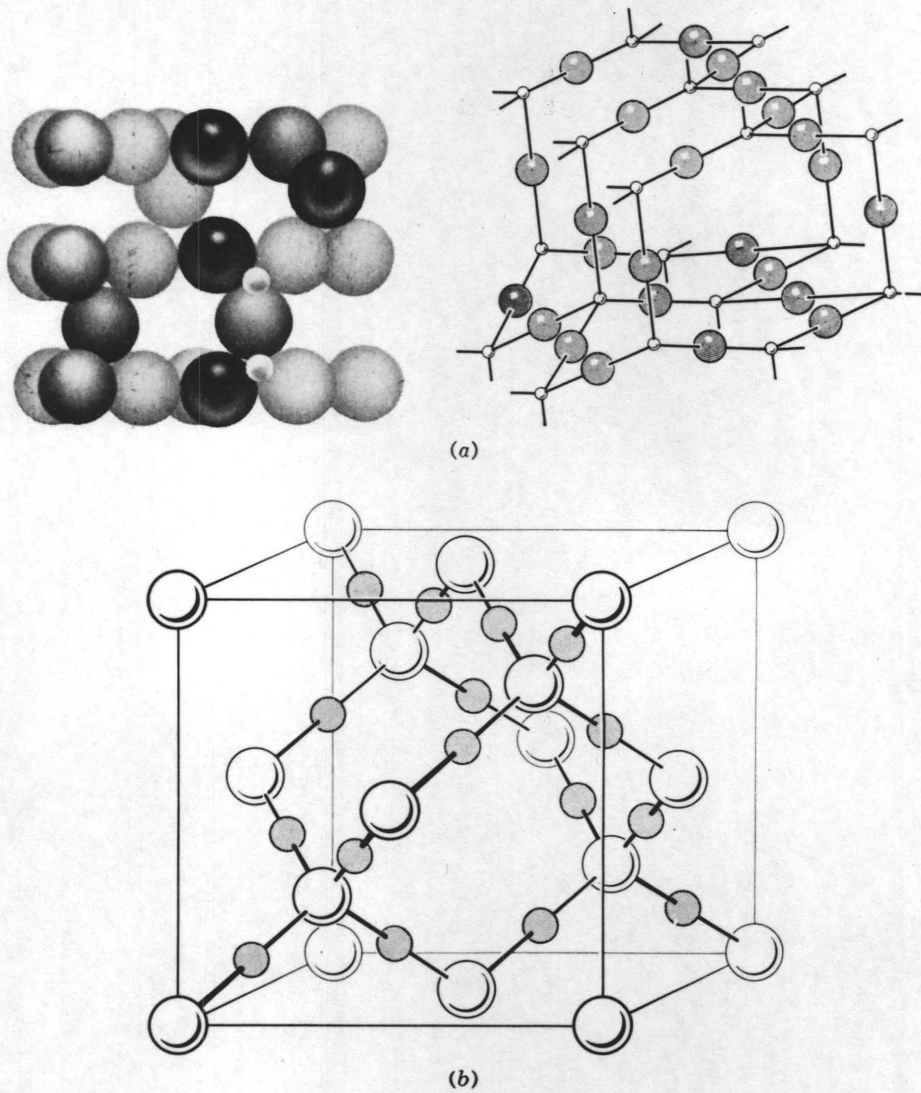
Figure I.4   Structures of
       a) high tridymite stable between 867 and 1470°C and
       b) high cristobalite stable between 1470 and 1710°C.

are present in nature and will tend to aid diffusion[13].

Mortley[14] has suggested that diffusion through quartz is limited to small univalent ions and occurs through lattice channels in the <0001> direction and also that these channels (of radius 1 $\overset{o}{A}$) act as an ionic sieve allowing only the smaller ions to pass. But, diffusion in quartz is not found to be restricted to ions with an ionic radius of 1 $\overset{o}{A}$ or less. White[13] diffused rubidium (ionic radius 1.49 $\overset{o}{A}$) and Cesium (ionic radius 1.65 $\overset{o}{A}$) into quartz. The fact that ionic movement through quartz occurs readily in the <0001> direction and not in any other direction, i.e., anisotropy of diffusion in quartz, was demonstrated by Frischat also[15,16] who followed the diffusion of radioactive ^{22}Na perpendicular to the <0001> direction. Residual γ activity was used to follow the diffusion. Frischat[17] also measured the diffusion of radioactive ^{45}Ca parallel to the c axis between 600° and 1000°C. His results are shown in Figure I.5. He describes the temperature dependence of the diffusivity of ^{23}Na in the <0001> direction as $D = 0.68 \exp(-20.2/RT)$ cm^2/sec., within the temperature range from 300° to 570°C. In comparison to the diffusion coefficient parallel, the diffusion coefficient perpendicular to the c axis direction was found to be 3 or 4 orders of magnitude lower. Between 600° and 820°C, the temperature dependence of the diffusion coefficient of calcium parallel to the c axis was described by the equation $D = 1 \times 10^{-5} \exp(-68 \text{ kcal}/RT)$ cm^2/sec. Within the temperature range from 820° - 1000°C no clear increase of the diffusion coefficient was observed. At 600°C, the diffusion of calcium parallel to the c axis is about seven orders of magnitude slower than sodium.

Silica frequently occurs in association with water. Ranging from the early studies of silica gel as a colloid system to present-day application as a drying agent, catalyst component and refractory, the
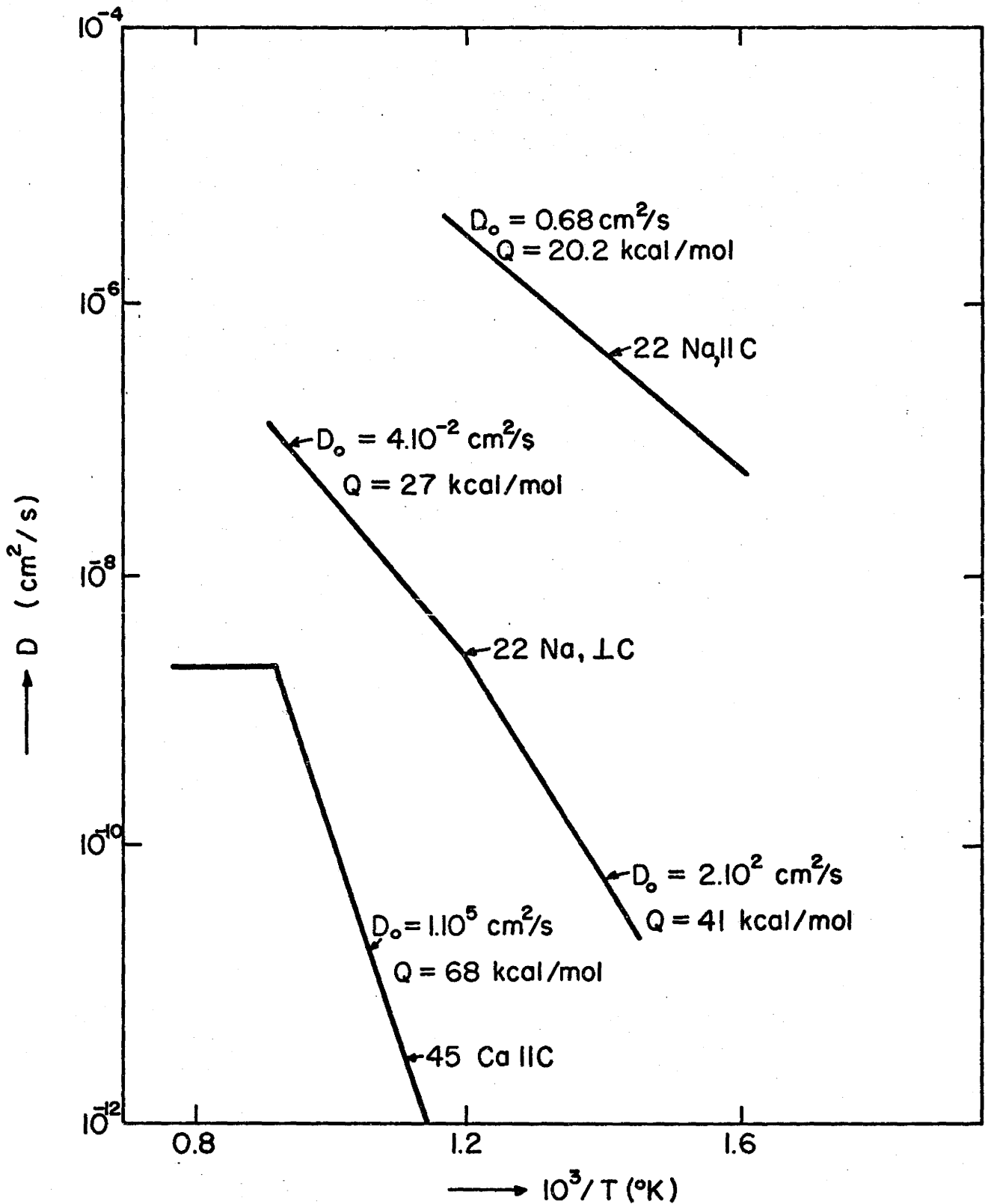
Figure I.5   Diffusion coefficient of radioactive [45]Ca parallel to the c axis as a function of temperature between 600° and 1000°C.

silica water system is of great importance.

All silica surfaces in contact with gaseous or liquid H_2O or with phases containing H_2O will not only react with OH^- ions but will also hold firmly a layer of H_2O of variable thickness. The contributions of the surface layers of OH^- and H_2O vary greatly between the amorphous and crystalline modifications of silica and also depend upon the previous history of the surface. Young[18] who studied the interaction of water vapor and silica samples showed that water vapor physically adsorbs on the silanol (hydroxyl) sites of the silica surface.

The fact that water vapor does not adsorb on silica surface which is void of silanol groups implies that the silicon oxygen surface bonds are homopolar in character. Physical adsorption of water vapor on the silica surface is restricted to the vicinity of silanol sites even at high relative water vapor pressures. Adsorption is initiated on the surface hydroxyl sites and probably proceeds by the building of adsorbed molecules around these sites. Heating to temperatures above 400° - 500°C removes the silanol sites from the surface and these cannot be re-hydrated by water vapor. Former silanol sites cannot be re-hydrated because physically adsorbed water vapor is needed to initiate the re-hydration. However, if this hydrophobic silica surface is exposed to bulk water, silanol sites are readily reformed.

Drury, Roberts and Roberts[19] have suggested one mechanism of water diffusion into silica glass. According to them, each water vapor molecule reacts with an $\equiv Si - O - Si \equiv$ bridge at the surface, giving a pair of silanol groups. Subsequent movement of water into the volume of the glass proceeds by a proton jump to a neighbouring internal $\equiv Si - O - Si \equiv$

bridge followed by the jump of an hydroxyl group. These two steps are then repeated continuously, giving a net transfer of H and O in the ratio 2:1, with formation of new pairs of hydroxyl groups and reformation of ≡ Si - O - Si ≡ bridges at each stage.

Utilising this mechanism, the following model has been suggested for solid solution of calcium in quartz[20]. Water molecules at the quartz surface initially proceed into the quartz by breaking the ≡ Si - O - Si ≡ bridges as described above. This leads to an "opening" of the structure and a consequent widening of the holes in the crystal making it easier for them to accommodate a larger ion.

C. Lime

Lime (CaO) has the cubic rocksalt structure (Figure I.6) with the large oxygen anions arranged in cubic packing and Ca^{+2} on all the octahedral interstitial sites.

D. Silicates

The binding mechanism in the molecular unit SiO_2, the tetrahedral unit co-ordination group SiO_4 and its tendency to polymerise into chains, networks, sheets and frameworks are fundamental facts on which the structural study of the silicates is based[21]. The tendency of the Si-O-Si groups
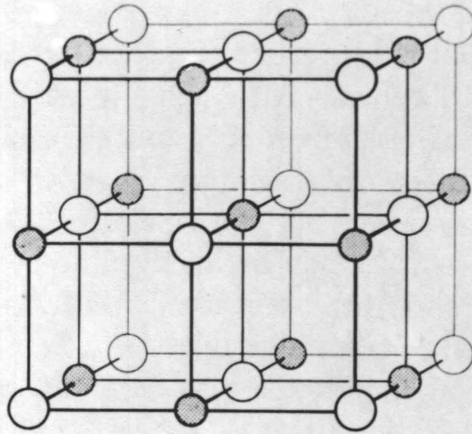
(a)
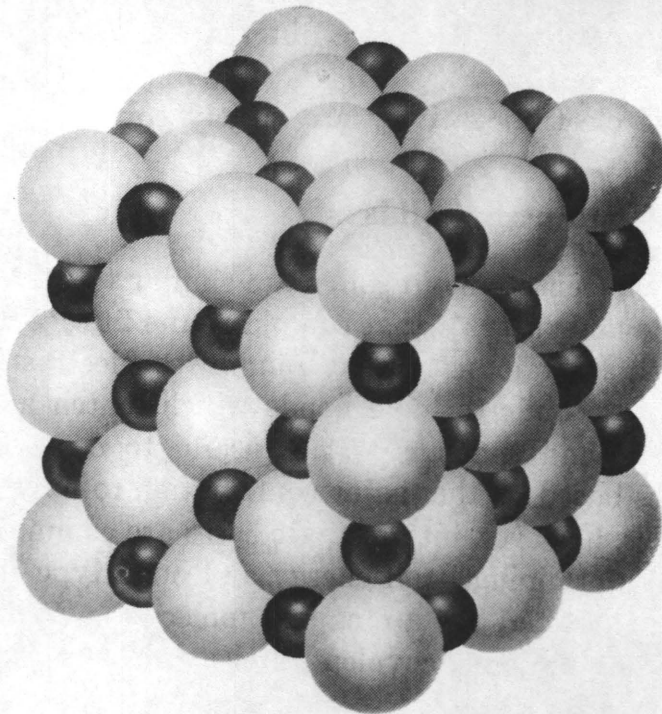
(b)

Figure I.6   Crystal structure of sodium chloride.

not to form stretched arrangements with an angle of 180° between the branches but angles of approximately 130° is well known. This fact is a powerful principle of selection of the particular interlinkages in tetrahedral SiO_4 arrangements.

Ramberg[22] examined the polarization of the oxygen anions in silicates as an important indicator of the stability of single silicates. There is a general rule that the larger the size of a noble gas type cation and the lower its electrostatic charge, the more stable is its silicate relatively to the appropriate free oxides. This is due to the polarization effects exerted on the O^{2-} anions by the resulting field surrounding the Si^{+4} cations and those of the additional metals. The Si^{+4} - O^{2-} bonds are strengthened and the cation $-O^{2-}$ bond is weakened when the oxides react to form the silicate.

By combining SiO_4^{4-} tetrahedra in various ways, the whole family of silicates can be formed. Some of the modes of combination are illustrated in Figure I.7. The charges on the silicate radicals decide the mineral species formed. The simplest silicate structure is that in which all the oxygen are linked to other cations. The structure is known as an "island structure" (sometimes called orthosilicates). Forsterite (Mg_2SiO_4) monticellite $(CaMg)SiO_4$, Mn_2SiO_4 (triphroite), phenacite (Be_2SiO_4) and zircon (Zr_2SiO_4) are examples of this group. The structure of Mg_2SiO_4 can be described as an infinite array of approximately close packed oxygen atoms with silicon in tetrahedral and magnesium in octahedral interstices.

Chain structures are formed when tetrahedra are linked end to end. The repeat unit is $(SiO_3)^{2-}$ and the mineral family so produced are termed

SiO_4^{4-}

$Si_2O_7^{6-}$

$Si_3O_9^{6-}$

$Si_6O_{18}^{12-}$

$(SiO_3)_n^{2n-}$ – pyroxene

$(Si_4O_{11})_n^{6n-}$ – amphibole
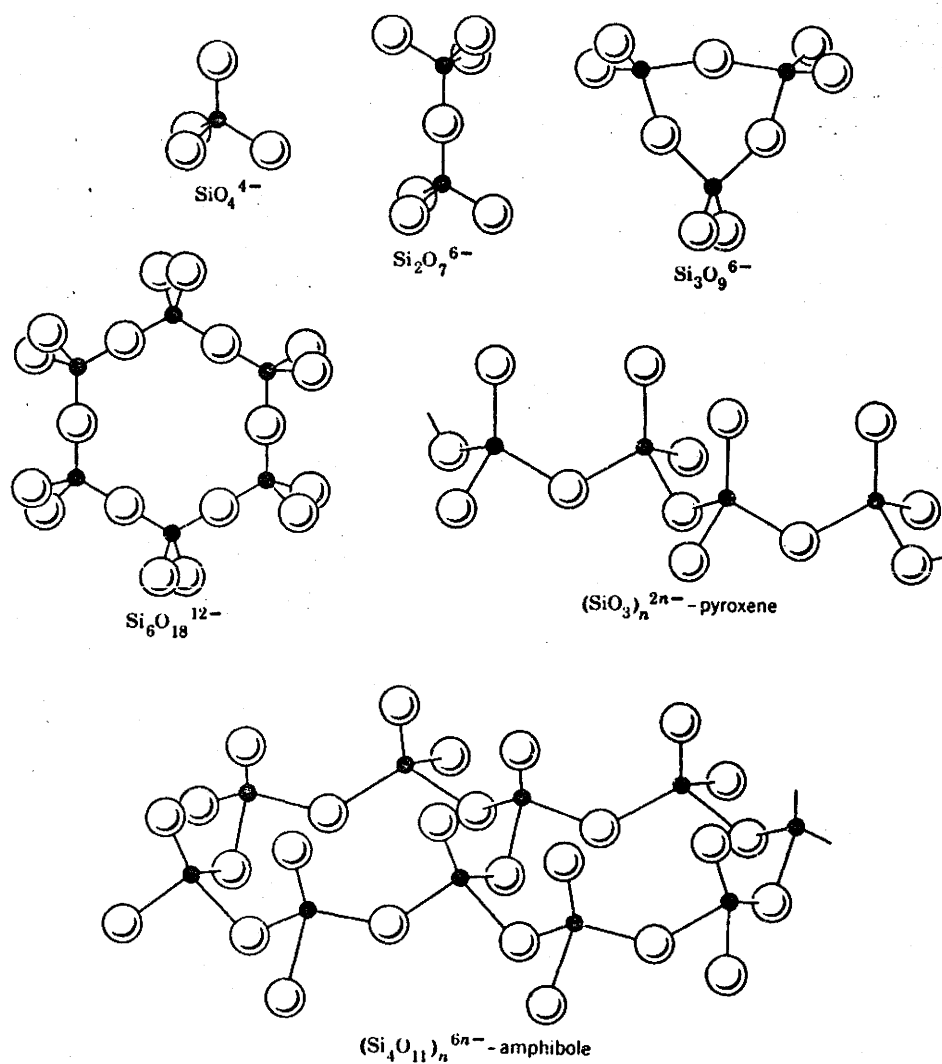
Figure I.7   Some silicate ions and chain structures.

pyroxenes. Some examples of pyroxenes are enstatite ($MgSiO_3$), wollastonite ($CaSiO_3$) and diopside ($CaMg(SiO_3)_2$). Two such chains can cross-link to give the amphibole minerals. One of the important amphiboles is tremolite ($Ca_2Mg_5(Si_8O_{22})(OH)_2$). Sheet structures are formed when the tetrahedra share sides and the repeat unit is $(Si_2O_5)^{2-}$. The clay mineral kaolinite, $Al_2(Si_2O_5)(OH)_4$, has this structure. Another clay system, an example of which is pyrophillite ($Al_2(Si_4O_{10})(OH)_2$), has two such sheets sandwiching a gibbsite sheet.

Lime and silica form four major silicate compounds, namely, calcium meta silicate (CS), dicalcium silicate (C_2S) and tricalcium silicate (C_3S) and tricalcium disilicate (C_3S_2). These are shown in the CaO-SiO$_2$ phase diagram in Figure I.8. Wollastonite ($CaSiO_3$) undergoes $\beta \rightarrow \alpha$ transition at 1125°C. Tricalcium silicate (C_3S) is found to be stable only between 1250°C and 1900°C[23]. Ca_2SiO_4 (C_2S) has four polymorphs of which two are high temperature forms (α' and α). The low temperature or γ form is very inert towards water. The β low temperature form, which is metastable at ordinary temperatures, reverts to the stable γ form with a large increase in volume and sets to a hard mass when finely ground and mixed with water. The γ form has olivine structure[24,25] and β form a monoclinic structure closely related to the α' form of C_2S[26,27].

The hydration of the calcium silicates is important in cement and ceramic technology. With the water cement ratios customarily used in cement pastes, mortars and concretes, tricalcium silicate hydrolyses, that is, breaks down to a calcium silicate of lower basicity ($2\,CaO.SiO_2$) and the excess lime is released as calcium hydroxide. Both the dicalcium silicate originally present in the cement and that resulting from hydrolysis of the higher lime
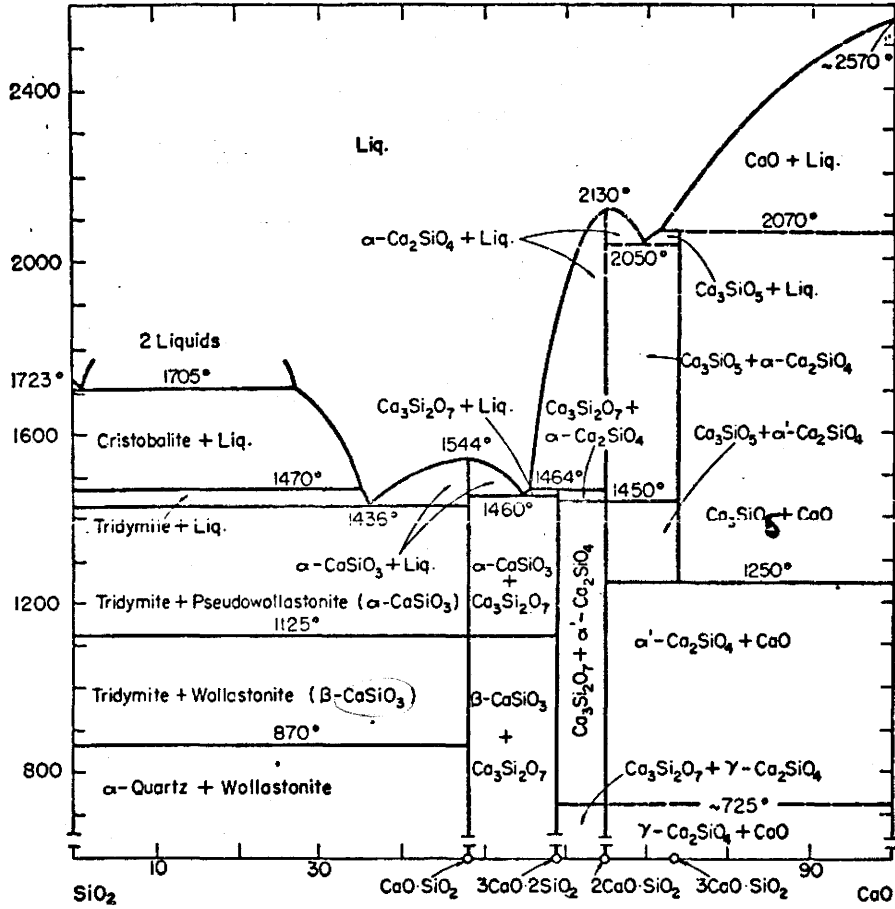
Figure I.8   System CaO-SiO₂.

compounds combine directly with water in a process called hydration.

Discrete tetrahedral groups, SiO_3OH^-, are found in afwillite[28] ($Ca_3(SiO_3OH)_2 \cdot 2H_2O$ or $3CaO \cdot 2SiO_2 \cdot 3H_2O$) and in dicalcium silicate α hydrate[29] ($Ca_2(SiO_3OH)OH$ or $2CaO \cdot SiO_2 \cdot H_2O$). Tricalcium silicate hydrate is $Ca_6(Si_2O_7)(OH)_6$. The crystals are hexagonal or trigonal. Xonotlite is $Ca_6(Si_6O_{17})(OH)_2$ or $6CaO \cdot 6SiO_2 \cdot H_2O$. Foshagite is $Ca_4Si_3O_9(OH)_2$, having infinite metasilicate chains similar to those in wollastonite. The fact that calcium silicate hydrates have characteristic chain silicate structures was described by Taylor[30]. Mamedov[31] determined Xonotlite to have a monoclinic structure with cell constants a = 16.95, b = 7.33, c = 7.63 A and $\beta = 90^\circ$. Megar and Kelsey[32] described the structure of tobermorite as very nearly orthorhombic with cell constants of a = 11.3, b = 7.37, c = 22.6 A forming a layer structure with layers parallel to <002> plane. The composition of tobermorite group is $CaO_{1-1.5} \cdot SiO_2 \cdot H_2O_{1-2.5}$ and is divided into 14 A, 11 A, 9A hydrates. Mamedov and Belov suggested a close structural resemblance between 11.3 A tobermorite and Xonotlite. Taylor[33] observed that a high degree of order is preserved in the transformation of tobermorite to Xonotlite.

The calcium oxide/silica reaction has been studied over a wide temperature range. The movement of Ca and Si in the liquid binary system was investigated by Majdic and Henning[34]. The diffusion was studied by electron microprobe analysis of the contact zone between plane ground ends of a pair of cylindrical specimens with compositions CaO/SiO_2, 33/17 and 57/43 at five temperatures between 1600 and 1700°C. In all the investigations on the solid state reaction between calcium oxide or carbonate and quartz, calcium orthosilicate is the first phase to form regardless of temperature and initial mole ratio of the reactants. In order to decide the order of appearance of

subsequent phases such as $Ca_3Si_2O_7$ and $CaSiO_3$, Jander and Hoffman[35] undertook a comprehensive investigation in which the effects of temperature, initial mole ratio of reactant, atmosphere and purity were systematically studied. Jander and Hoffman confirmed that C_2S ($2CaO \cdot SiO_2$) was always the first phase to appear. They summarised the whole sequence during the solid state reaction between CaO and SiO_2 as follows:

"A thin film of calcium orthosilicate forms between CaO and SiO_2. For the further reaction to proceed, CaO must be more mobile than SiO_2 through $2CaO \cdot SiO_2$. So long as there is excess of CaO and the temperature is sufficientl; high, there is hardly any formation of low order basic compounds on the ortho-silicate-silica boundary. As long as temperatures are not above $1300^{\circ}C$, there cannot be any, or very little, development of the higher order basic compound $3CaO \cdot SiO_2$ at the $CaO - 2CaO \cdot SiO_2$ interface. If there is no excess of lime and the temperature is low, diffusion will be slow and there is a possibility of development of $3CaO \cdot 2SiO_2$ and $CaO \cdot SiO_2$ on the boundary area of orthosilicate and silica, respectively".

Many workers have studied the system $CaO-SiO_2-H_2O$. Literature concerning this system (back to 1947) has been reviewed by Steinour[36].

Taylor[37] identified the products of the system and established phase equilibria data for hydrous calcium silicates in contact with lime solutions. The processes in the interaction of lime solutions with silica particles at 30° to $85^{\circ}C$ were described by Greenberg[38] as follows:

a) Chemisorption of lime on the surface of silica.

b) Solution of Silica to form, in turn, H_4SiO_4, $H_3SiO_4^-$, $H_2SiO_4^{--}$ with increasing pH.

c) Reaction of monosilicic acid with Ca^{+2} ions in the solution.

d) Formation of nuclei of calcium silicate hydrate.

e) Growth of these nuclei.

f) Precipitation of crystals of calcium silicate hydrate.

Greenberg found the solution of silica to be the rate determining step whereas other workers found evidence that the overall reaction was diffusion controlled. Logginov[39] et al, however, believe that a film of product surrounded the silica particle, reached a maximum thickness and remained unchanged. The kinetics of solution of quartz and the crystallisation of calcium silicate hydrate during hydrothermal treatment of single crystals of quartz in saturated lime solutions were studied by Moorhead and McCartney[40]. Microscopic examination of sections of the product layer showed that the calcium silicate hydrate was of fibrous crystal habit and grew radially from nucleating centres in a general direction away from the quartz surface. The product layer was extended only on the surface in contact with the lime solution. The silicate ions apparently diffused preferentially through the product layer, although separate measurements proved that the membrane had no selective action against the diffusion of calcium ions. At 235° and $335^{o}C$, plots of weight of the calcium silicate hydrate vs. square root of time gave straight lines indicating that the process was diffusion controlled.

The kinetics of solid state reaction between CaO and SiO_2 in dry atmospheres or in the presence of moisture, at relatively high temperatures, has been a subject of interest to many workers. Jander and Hoffman[35] determined the relative amounts of Ca_2SiO_4, $Ca_3Si_2O_7$, and $CaSiO_3$ as a function of time at temperatures of 1000° to $1200^{o}C$. Jander[41] theorised a parabolic reaction rate for the $CaO-SiO_2$ reaction but did not confirm his thoughts

experimentally. He concluded that the rate but not the course of reaction, was enhanced markedly in the presence of water vapor. In studies of the reaction at low temperatures, Kakitani and Fukisaka[42] found that after 272 hours at 700°C, the only product identifiable by X-ray was Ca_2SiO_4.

Verduch[43], in his study of the reaction between calcium carbonate and cristobalite at temperatures between 500° and 700°C, suggested that the solid solution of calcium ions in cristobalite is an important part of the initial reaction mechanism. The reaction, according to him, proceeds in the following sequence:

1. Migration of ions of calcium from the calcium carbonate phase to the interior of the cristobalite phase.

2. Shortly after the dissolution process starts, a high concentration of Ca^{+2} exists near the crystal surface, the interior concentration being very dilute. The oversaturation of the solid solution in the surface causes precipitation of the first nuclei of calcium ortho-silicate.

3. The orthosilicate layer grows by diffusion of Ca^{+2} and at the same time, the solid solution of CaO in cristobalite proceeds.

4. When all the $CaCO_3$ available has been consumed, the flow of ions of calcium to the interface SiO_2-Ca_2SiO_4 is restricted. This is favorable condition for the appearence of the less basic silicates.

Under these conditions, the solid solution of calcium oxide in cristobalite is no longer stable. The ions of calcium emigrate from the interior of the solid to the SiO_2-Ca_2SiO_4 interface, and contribute to the formation of $Ca_3Si_2O_7$ and later $CaSiO_3$[44]. It is believed, therefore,

that the ex-solution of calcium oxide plays an important role in the nucleation and initial growth of the crystals of $Ca_3Si_2O_7$ and $CaSiO_3$. The solution finally reaches a state of extreme dilution and further growth of the final phase $CaSiO_3$ must be done entirely from the $Ca_3Si_2O_7$ and Ca_2SiO_4 products.

Montierth, Gordon and Cutler[45] made a kinetic study of the $CaCO_3$-SiO_2 reaction utilising a thermogravimetric technique, particularly suitable for reaction at temperatures between 700^oC and 850^oC. By conducting the reaction in a CO_2 atmosphere and at temperatures below that of the decomposition of calcium carbonate, it was possible to attribute the measured weight loss to the actual reaction between the calcium carbonate and quartz, on the formation of the silicate product. Finely powdered quartz and $CaCO_3$ powder were pressed into pellets and reacted at temperatures between 700^oC and 850^oC. The following reaction took place:

$$2CaCO_3 + SiO_2 \rightarrow Ca_2SiO_4 + 2\ CO_2$$
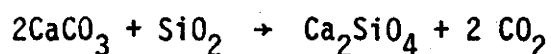
They reached the following conclusions:

1. The solid state reaction between calcium carbonate and quartz, as determined by a standard thermogravimetric technique, occurs in two distinct steps. The initial portion is believed to be the solid solution of calcium into the quartz and the final stage, which follows a parabolic reaction kinetics, is believed to be a diffusion controlled process in a well defined product layer.

2. The initial reaction is enhanced markedly in the presence of water vapor in the reaction atmosphere or as adsorbed water on the surface of the calcium carbonate reactant particles.

3. The proposed solid solution of calcium into quartz is enhanced by water vapor.

4. The parabolic portion of the reaction is probably controlled by the diffusion of calcium ions through the product layer (Figure I.9).

Verduch did not consider the effect of water vapor on the $CaCO_3$/ cristobalite reaction. Montierth, Gordon and Cutler considered the effect of water, but did not observe any reaction layer in the samples so reacted. They did, however, observe a definite calcium concentration in the quartz particles. According to Verduch, upon reaching a critical value of 0.08% CaO in silica, the orthosilicate phase was nucleated. If, as Taylor suggests, water diffuses into quartz breaking Si-0 bonds and opening the structure making it easier for Ca^{+2} to diffuse into silica, one could expect a corresponding critical value of CaO concentration in wet atmosphere-reacted samples. The enhanced kinetics of calcium solid solution in wet atmosphere conditions, might be expected to bring about earlier nucleation of the silicate in the wet than in the dry case. Montierth et al did not determine whether water vapor influences the reaction after nucleation of the calcium orthosilicate layer.

Jander and Hoffman and Montierth et al used silica and CaO or $CaCO_3$ powders to study the solid state reaction. Jander and Hoffman heated pulverised mixtures of $CaCO_3$ and SiO_2 powders in a platinum crucible for 0, 3, 6, 10, 24 and 48 hours at temperatures between 1000° and 1200^oC and found the relative amounts of $2CaO \cdot SiO_2$, $3CaO \cdot 2SiO_2$ and $CaSiO_3$ as a function of time. They did not consider the effect of water vapor on the reaction nor did they consider the possible influence of the crystallographic direction in the quartz on the reaction kinetics. On the other hand, Montierth et al did consider the
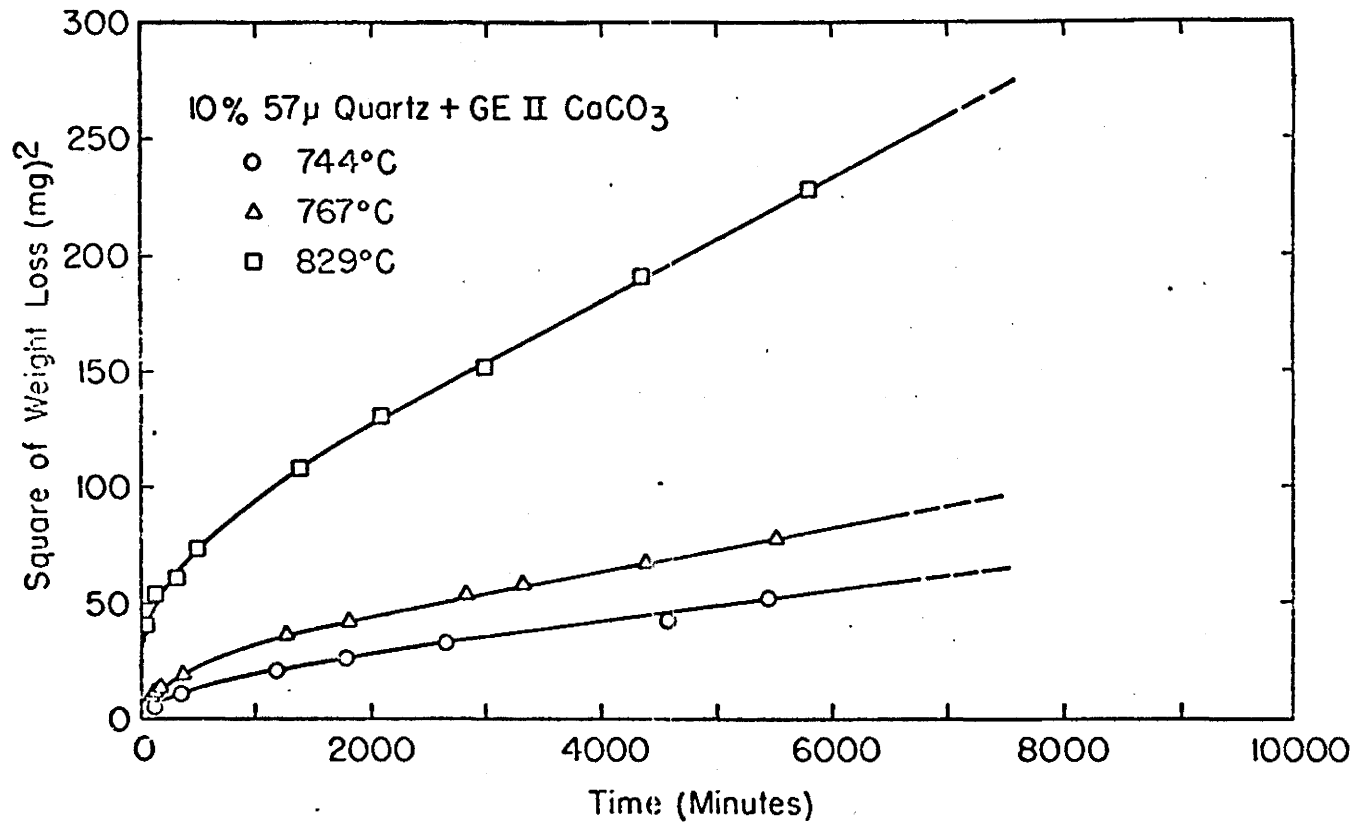
Figure I.9 (a) Parabolic rate plot for 57 μ quartz + GE 11 CaCO₃ reacted in dry CO₂.
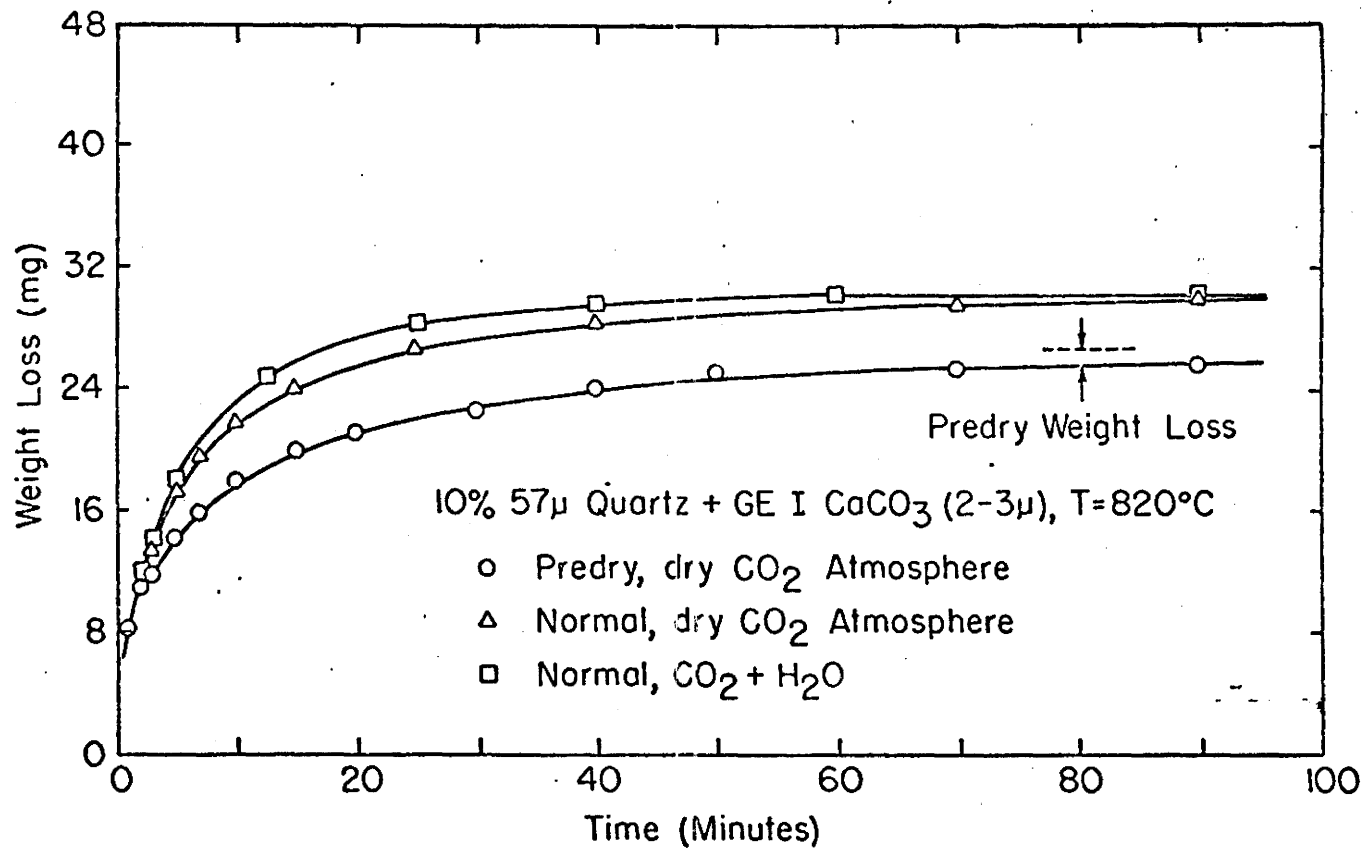
Figure I.9 (b)   Effect of water vapor on the initial reaction.

influence of the water vapor on the calcium diffusion rate but not as a function of quartz crystallographic direction either. The diffusion of cationic species in quartz is highly anisotropic. It is probable, therefore, that the $CaO-SiO_2$ reaction is also highly dependent on the orientation of the SiO_2 crystal. It is evident that a systematic study of the kinetics of the solid state reaction between CaO and SiO_2 needed to be undertaken in the temperature range 1000° - 1200^oC, taking into account the effect of the presence of moisture in the atmosphere and of different quartz crystallographic directions on the cationic diffusion and product layer development rates. This was achieved in the present investigation by reacting pellets of CaO and single crystal quartz at temperatures of 1000^oC, 1050^oC, 1100^oC, 1150^oC and 1200^oC in wet and dry nitrogen atmospheres. The concentration profiles obtained on the electron microprobe analyser always indicated the formation of only one silicate, i.e., dicalcium silicate, on any crystallographic plane in both wet and dry atmospheres. Excess lime was always present and only dicalcium silicate was formed. The development of the silicate layer on different crystallographic planes of quartz in wet and dry atmospheres as a function of time and temperature was studied.

EXPERIMENTAL PROCEDURE

A. Apparatus

A Kanthal wound horizontal electric furnace (Figure II.1) was
used in all the experiments. Temperatures were controlled to within $\pm 4^{\circ}C$
using an on/off controller and a Pt-13% Rh thermocouple in the hot zone of
the furnace. With the furnace operating under the same conditions as the
actual runs, the hot zone was found to be approximately 2½" long. Tempera-
ture measurements were made on Rubicon Model 2710 A potentiometer. The
sample inserting assembly consisted of an alumina sample boat with an
alumina tube extension. The alumina tube was connected rigidly to the
alumina sample boat by kanthal wire. The total length from one end of the
alumina boat to the other end of the extension was 1'5" as shown in Figure II.2.

Experiments were carried out in an impervious open-ended mullite
tube of 1½" ID and 3' in length. The length of the furnace tube was 2', so
that the mullite tube could be closed at both ends by rubber stoppers even
at hot zone temperatures of $1200^{\circ}C$. To insert 8 samples at the same time,
insulating bricks were shaped as shown in Figure II.3. The total length of
the rail assembly left a clearance of 1" at each end of the mullite tube.
This arrangement allowed rubber stoppers to be inserted at both ends. The
rubber stoppers carried glass tubes for wet and dry nitrogen and a thermo-

Figure II.1   Diagram of furnace.

1. Thermocouple for measuring the sample temperature
2. Insulating brick which creates 4 compartments in the furnace tube
3. Mullite tube used for running controlled atmosphere
4. Control thermocouple
5. Gas inlet
6. Gas outlet
7. Fibre frax insulation
8. Insulation bricks
9. Mullite core tube for heating elements
10. Heating elements
11. Insulating brick to support the mullite tube
12. Rubber stopper
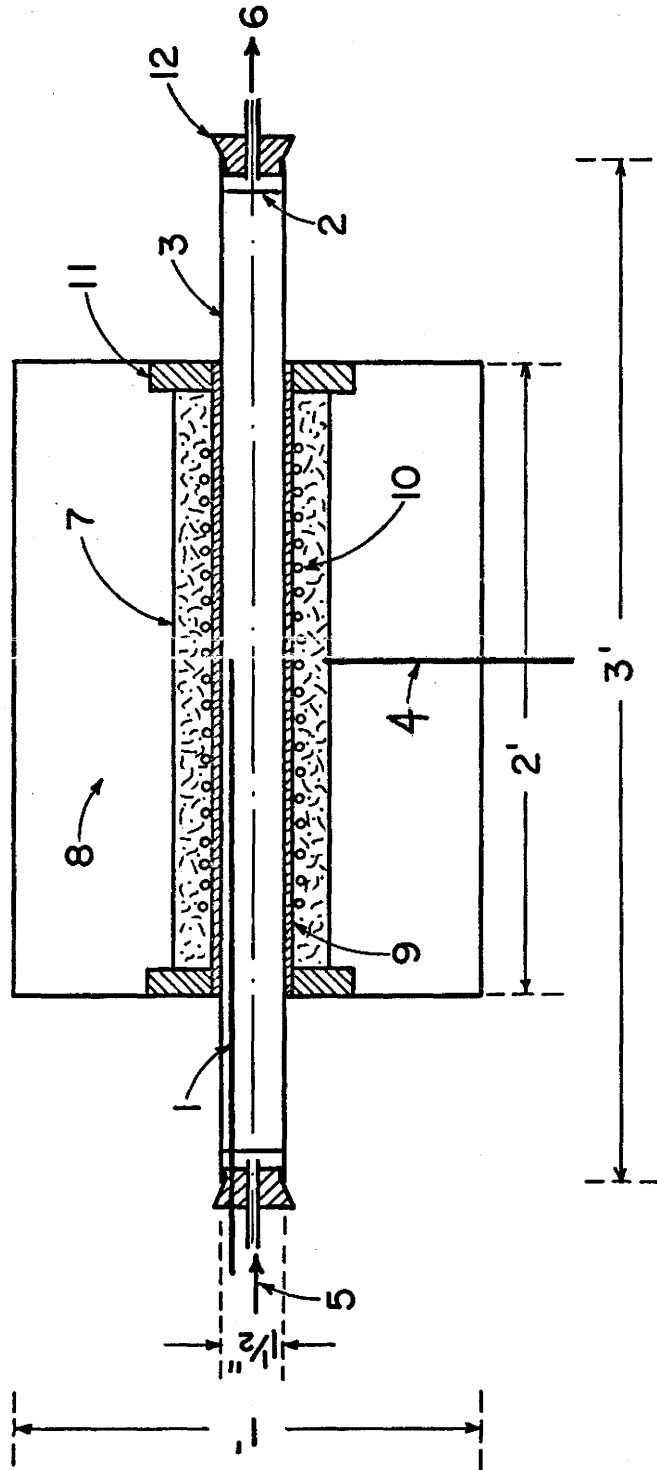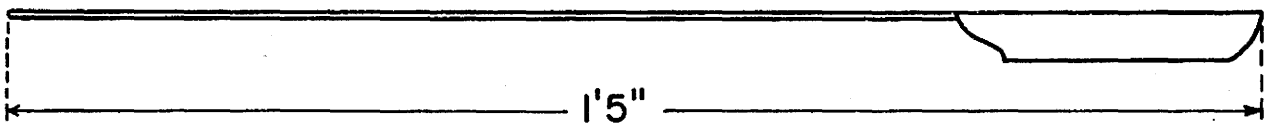
Figure II.2   Sample boat.
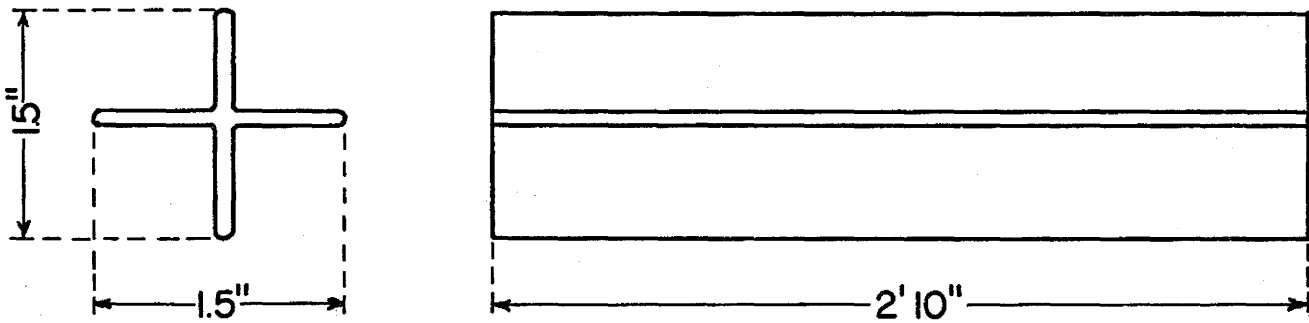
Figure II.3   The insulating brick in the furnace tube.

couple to measure the sample temperature. In the four compartments, 8 sample boats were inserted, four from each end with the sample pellet located in the end of each boat.

The nitrogen used was standard dry nitrogen of 99.9% purity obtained from "Liquid Air Canada". For the investigations carried out in dry atmospheres, the nitrogen was further dried through two columns of drierite and a flask containing sulphuric acid. Drierite (size 8 mesh and chemical formula $CaSO_4$) was supplied by W. A. Hammond Drierite Company. In the wet nitrogen experiments, the gas was passed through distilled water at $70^{o}C$. Distilled water was heated and maintained at $70^{o}C$ by heating the water-containing flask on a Thermolyne plate heater.

B. Sample Material and Preparation

The quartz crystals used were high purity, radio quality Brazilian quartz. Quartz single crystals of dimensions 3 mm x 1½ mm x 2 mm were cut from a single crystal plate on a micromatic precision wafering machine (model WMSA #2854). The 1½ mm x 2 mm faces were cut parallel to the crystallographic basal plane and 1½ mm x 3 mm faces were cut parallel to the prism planes. The quartz single crystal plate was mounted on a graphite disc with thermo-setting resin. Quartz pieces were then cut by a diamond wheel 5" in diameter, 5/8" bore and 19 thou in thickness. The crystal pieces were removed from the graphite block by heating and softening the resin. The residual resin

was removed from the quartz pieces thus:

i)   the crystal pieces were washed in a soap solution for 15 minutes,

ii) soaked with acetone in an ultrasonic cleaner for half an hour,

iii) soaked in concentrated sulphuric acid for 24 hours,

iv) and the acid washed off thoroughly and clean pieces obtained.

X-ray diffractometer traces were obtained for quartz in the temperature range between 1000^oC and 1200^oC. A portion of X-ray diffractometer trace for quartz reacted at 1200^oC for 24 hours and cooled to room temperature is shown in Figure II.4 . CuKα radiation was used with chart speed of $\frac{1}{2}^o$ per minute. Peaks 1 and 2 are major α-quartz reflections with d spacings of 4.28 and 3.343 A^o respectively. Peak 3 is a tridymite reflection. This diffractometer trace indicates that in the temperature range between 1000° and 1200^oC, β-quartz was the major phase with small minor amounts of tridymite. This observation was confirmed by high temperature X-ray rotation diffraction patterns.

The calcium oxide powder used was Fisher Certified Quality and it was heated in an oven at 1050^oC for 24 hours to remove adsorbed moisture. The powder was then stored in a desicator until used.

Carefully pressed pellets of CaO/SiO_2 with a centrally located quartz crystal were pressed at 56000 psi in 0.9 cm die (drill rod pins of hardness RC 45 and bore of hardness RC 59). The samples were immediately transferred to a desicator following pressing. The sample pellet weight was always 1 gram.

Marker experiments were performed by putting markers on the quartz surface in contact with CaO. The position of the markers after reaction
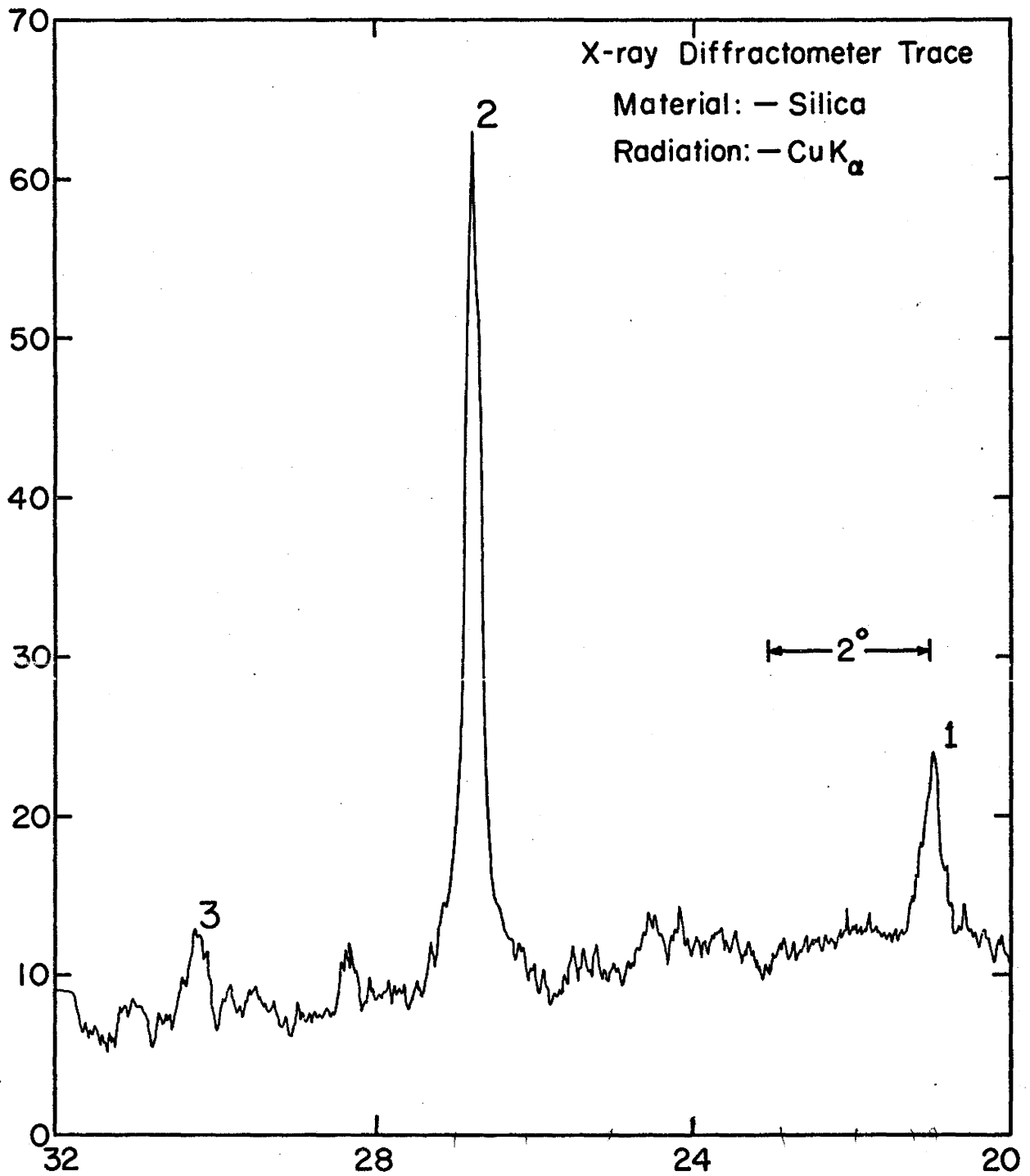
Figure II.4   Diffractometer trace for silica.

in wet and dry atmospheres gave information about the mechanism of reaction. The markers used were derived from platinum paste (Engelhard Hanovia Liquid Gold Division, East Newark, N.J., platinum paste lot #13096). The surfaces of quartz to be coated with platinum paste were polished to 0.02 μ and cleaned of grease. The absolutely dry pieces were then coated with the paste in the desired region. The prepared crystals were then dried in air and fired in a furnace at $500^{\circ}C$ to burn off the organic component of the paste. A firm coating was thus obtained on the quartz surface and it served as an experimental marker. Sample pellets containing quartz with platinum markers were pressed following the usual procedure. The samples with markers were reacted in the same manner as those without markers.

C. Experimental Procedure

All the runs were made in wet or dry nitrogen atmospheres. The system was first flushed with nitrogen for 10 minutes and the eight samples (four from each side) were introduced into the predetermined hot zone of the furnace. The nitrogen flow rate for all the runs was kept at 60 ± 3 bubbles/30 seconds. Samples were extracted from the furnace after known times of reaction at known temperatures. Sample removal time was kept at a minimum (< 1 minute) and it is not considered that these transitory periods influenced the remaining samples unduly. Samples were cooled slowly through $573^{\circ}C$ and no significant cracking was observed. The sample

heating time was estimated to be about three minutes.

The samples obtained after reaction were quite fragile and in order to bind, section and examine them, it was necessary to impregnate them with epoxy resin. The impregnation assembly is shown in Figure II.5 . The sample was put in a paper cup in a desicator maintained under vacuum by a mechanical pump. The epoxy resin was put in the separating funnel (2) with the stopcock (3) closed. When the desicator was evacuated, it was isolated from the mechanical pump by closing the stopcock (4) and simultaneously opening stopcock (3). The epoxy was drawn into the assembly and was allowed to cover the sample. The subsequent introduction of atmospheric pressure forced the epoxy into the sample. The samples were left in the resin for some time and then removed and allowed to harden overnight. The hard epoxy maintains all the reaction components in their experimental configurations, protects them from the atmosphere and allows the pellet to be sectioned satisfactorily.

The resulting samples were sectioned and mounted in lucite. They were then polished on silicon carbide grits 270, 325, 400 and 600 and on diamond polishing pads to 1 micron. The samples were finally polished to 0.3 μ Al_2O_3 on a Sintron vibrating polisher. The samples were then ready for microscope and electron microprobe examination.

D. Sample Analysis

Electronprobe microanalysis is nondestructive, can be used to analyse accurately positioned volumes of material of $\sim$ 1 μm dia. with a sensitivity of
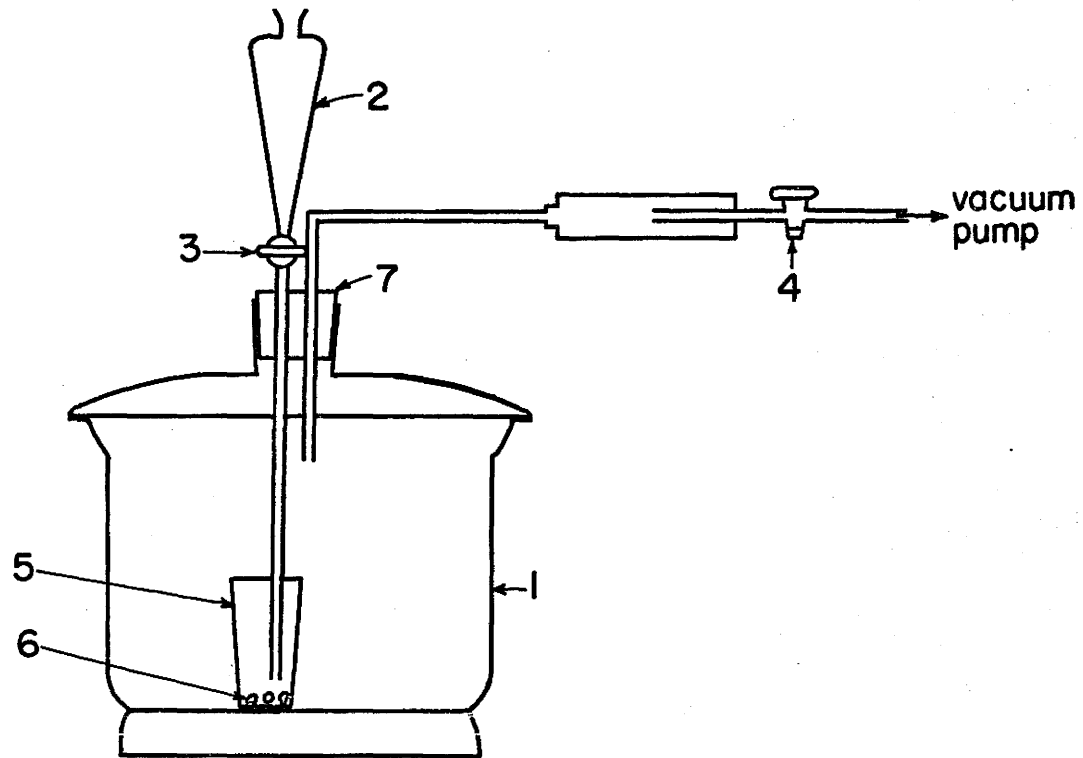
Figure II.5   The impregnation assembly.

1. Desicator
2. Separating funnel with a long end
3. One-way stopcock to let in epoxy resin with hardener
4. One-way stopcock to connect or isolate the vacuum pump
5. Paper container
6. Samples
7. Rubber stopper with 2 holes

100 ppm or an accuracy better than 1%, can give information about the distribution of species over the surface and in depth of almost all the elements with a few exceptions. It also requires a minimum of sample preparation.

An Acton microprobe was used to obtain line scans for distribution of calcium and silicon across the prepared samples. Calcium and silicon concentration profiles across the sample were thus obtained. These concentration profiles gave information on the following points:

i) whether more than one silicate was formed at any time in either wet or dry atmospheres on different crystallographic planes of silica. (Dicalcium silicate (molar ratio $CaO:SiO_2$ of 2:1) was verified as the only silicate that formed.),

ii) the thickness of the silicate layer in both wet and dry atmospheres on the basal and prism planes of quartz,

iii) the extent of calcium penetration into the quartz and whether it differs   a) in different crystallographic directions

        b) in wet and dry atmospheres,

iv) some indications of the possible mechanism of formation of the first silicate layer, the composition of which was determined by the point counts taken on the product layer.

The line scans were obtained for all the reacted samples at 1000, 1050, 1100, 1150 and 1200°C for 15, 30, 45 minutes and 1, 2, 6, 12, 16, 20 and 24 hours.

A Zeiss Cameramicroscope Ultraphot II was used for optical microscopic examination and product-layer thickness measurements on the samples.

A well-focused image of the sample on the projection screen was used to determine the thickness of the product layers. The exact magnification was found by projecting the accurately known distance on the projection screen. The thickness of the silicate layer formed on a particular plane of silica was determined by sectioning the sample perpendicular to that plane and making the thickness measurements at the five maximum points. The average of these measurements was taken to be the thickness of the product layer. Good agreement was observed between the thickness of silicate layer measured on the microscope and the thickness of the product (silicate) layer indicated by the concentration profiles obtained on the electron microprobe. Microscopic examination of the samples with platinum markers on desired faces of the quartz crystals, revealed the final position of the markers after reaction.

Some samples were impregnated and cut in the usual fashion and mounted on a glass plate with thermosetting resin for thin section fabrication. The samples were then ground in a thick slurry of 600 grit silicon carbide on a glass plate. The thin sections were then examined in transmitted polarised light and coloured micrographs were obtained.

CHAPTER III

RESULTS AND DISCUSSION

A. Kinetic Data

The kinetics of the solid state CaO/SiO_2 reaction under dry conditions and the enhancement thereof in the presence of moisture can be studied by plotting the thickness of the product layer formed on the specific crystallographic plane of silica as a function of time and temperature of reaction under both conditions. The literature regarding the phase transformations of silica and the present X-ray diffraction study of quartz single crystals indicated that in the temperature range of interest, β-quartz was the major phase present with small minor amounts of tridymite. It is assumed in the following analysis that small amounts of tridymite present do not influence the CaO/SiO_2 solid state reaction significantly and the silica phase present, is, therefore, assumed to be β-quartz. The excess CaO always present in the samples ensured the formation of C_2S (dicalcium silicate) only and the electron microprobe data indicated the molar ratio of $CaO:SiO_2$ in the reaction product was very nearly 2:1 in every case.

Plots of the square of thickness in μm of the product layer (C_2S) developed on the (0001) basal plane of β-quartz reacted with CaO at

1200, 1150, 1100 and 1050°C are shown in Figures III.1, III.2 and III.3 respectively as a function of the time in hours of the reaction. Figures III.4, III.5 and III.6 show plots of the square of the thickness of silicate layer in μm as a function of time (hours) of reaction on the ($10\bar{1}0$) β-quartz prism planes in wet and dry nitrogen atmospheres at 1200, 1150, 1100 and 1050°C respectively. Comparison plots of the square of C_2S layer thickness (x^2) on the basal and prism planes of β-quartz in wet and dry nitrogen atmospheres at 1200, 1150, 1100 and 1050°C are shown in Figures III.7 and III.8 respectively as a function of time (hours).

The square of the silicate thickness developed as a result of the CaO/SiO_2 solid state reactions is a linear function of the time of reaction after an initial deviation. The kinetics of the reaction between β-quartz and calcium oxide at these temperatures, therefore, appear to obey the parabolic rate law with an initial non-parabolic period. The species transfer through the product (C_2S) layer is probably, therefore, the rate controlling step.

In the temperature range between 1000°C and 1200°C, the presence of moisture in the atmosphere enhances the reaction between calcium oxide and β-quartz. Though the chemical composition of the product (molar ratio $CaO:SiO_2 = 2:1$) developed is the same, the thickness of the product is greater in the presence of moisture. This is very clearly evident in Figures III.1, III.2 and III.3. Twelve hours of reaction at 1200°C in a wet atmosphere showed a product layer of 30 μm thickness on the basal plane of β-quartz whereas in a dry nitrogen atmosphere the thickness was 20 μm. Reaction at 1050°C for 12 hours produced 11 μm's of product layer on the basal plane in wet and 7 μm's in dry atmospheres.

Figure III.1   Growth of C_2S on basal plane of β-quartz at $1200^{\circ}C$

in wet and dry nitrogen atmospheres.

CaO/β quartz basal plane reaction

1200 °C.

○ wet N_2 atmosphere

▲ dry N_2 atmosphere

BASAL PLANE

(THICKNESS OF C_2S)^2 μm^2

TIME (hours)
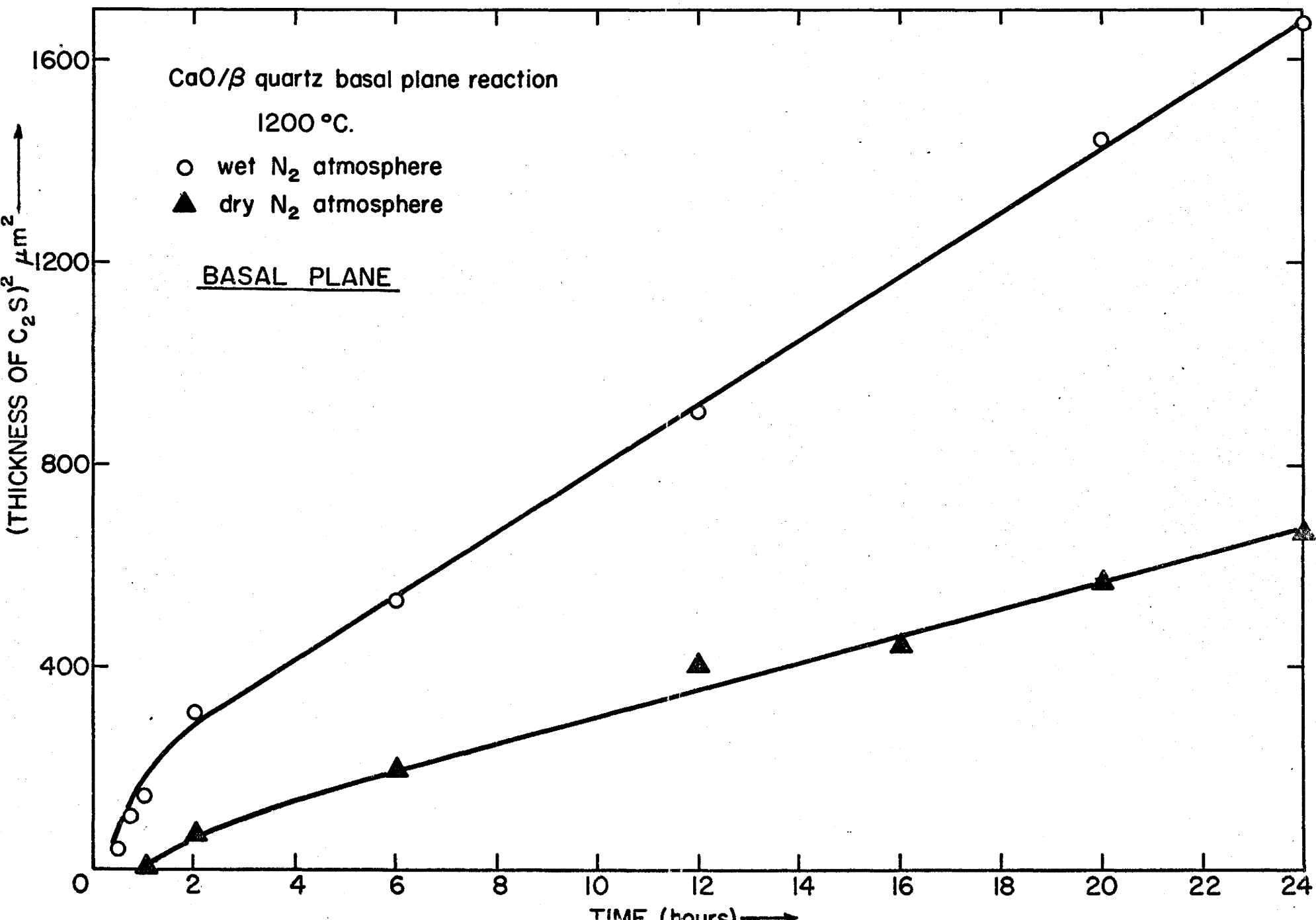
Figure III.2   Growth of C_2S on basal plane of β-quartz at $1150^{\circ}C$ in wet and dry nitrogen atmospheres.

CaO/β quartz basal plane
1150 °C
$\triangle$ Wet N_2 atmosphere
● Dry N_2 atmosphere

BASAL PLANE

(THICKNESS OF C_2S)^2 μm^2

TIME (hours) →
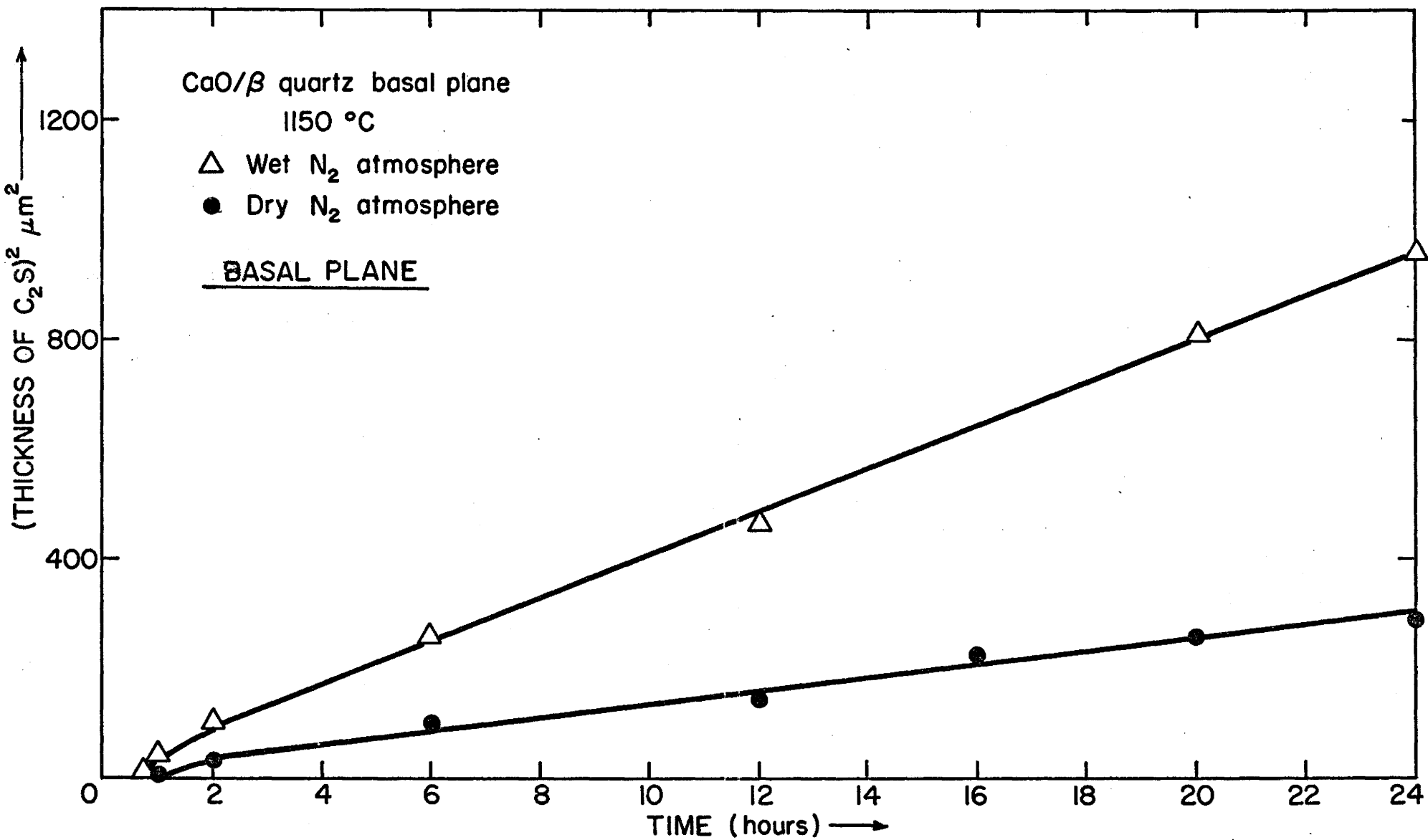
Figure III.3   Growth of C_2S on basal plane of β-quartz at 1100°C and 1050°C in wet and dry nitrogen atmospheres.

CaO/β quartz basal plane

○ 1100°C , wet N_2 atmosphere
▲ 1100°C , dry N_2 atmosphere
△ 1050°C, wet N_2 atmosphere
● 1050°C, dry N_2 atmosphere

BASAL PLANE

(THICKNESS OF $C_2S)^2$ μm^2

TIME (hours) ⟶
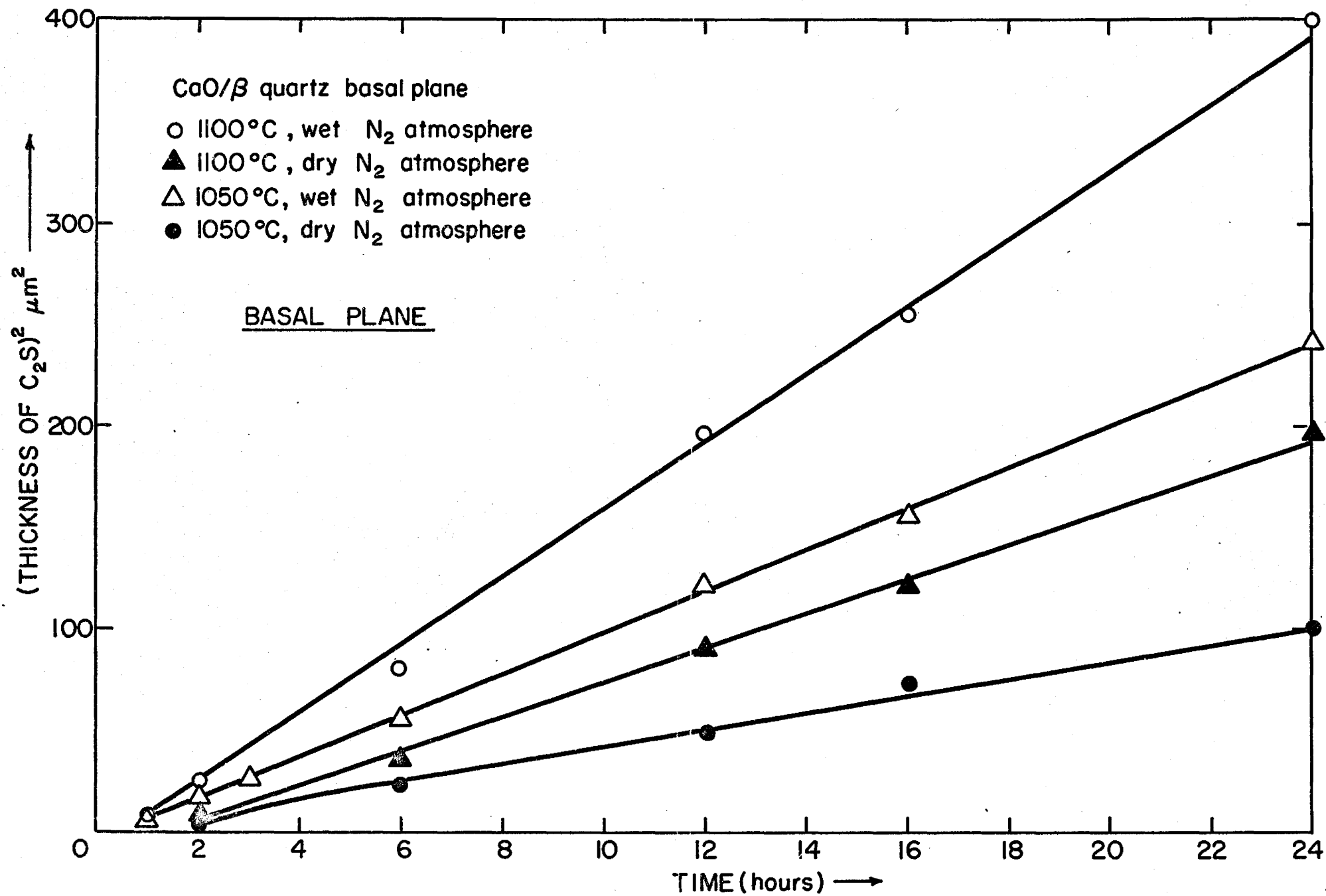
Figure III.4 Growth of C_2S on prism plane of β-quartz at 1200^oC

in wet and dry nitrogen atmospheres.

CaO/β quartz prism phase

1200°C.

△ wet N_2 atmosphere

○ dry N_2 atmosphere

PRISM PLANE

(THICKNESS OF C_2S)^2 μm^2

TIME (hours)

Figure III.5 Growth of C_2S on prism plane of β-quartz at
1150°C in wet and dry nitrogen atmospheres.

PRISM PLANE

CaO/β quartz prism plane

○ 1150 °C wet nitrogen atmosphere

△ 1150 °C dry nitrogen atmosphere

Y-axis: (THICKNESS OF C_2S)^2 μm^2

X-axis: TIME (hours)
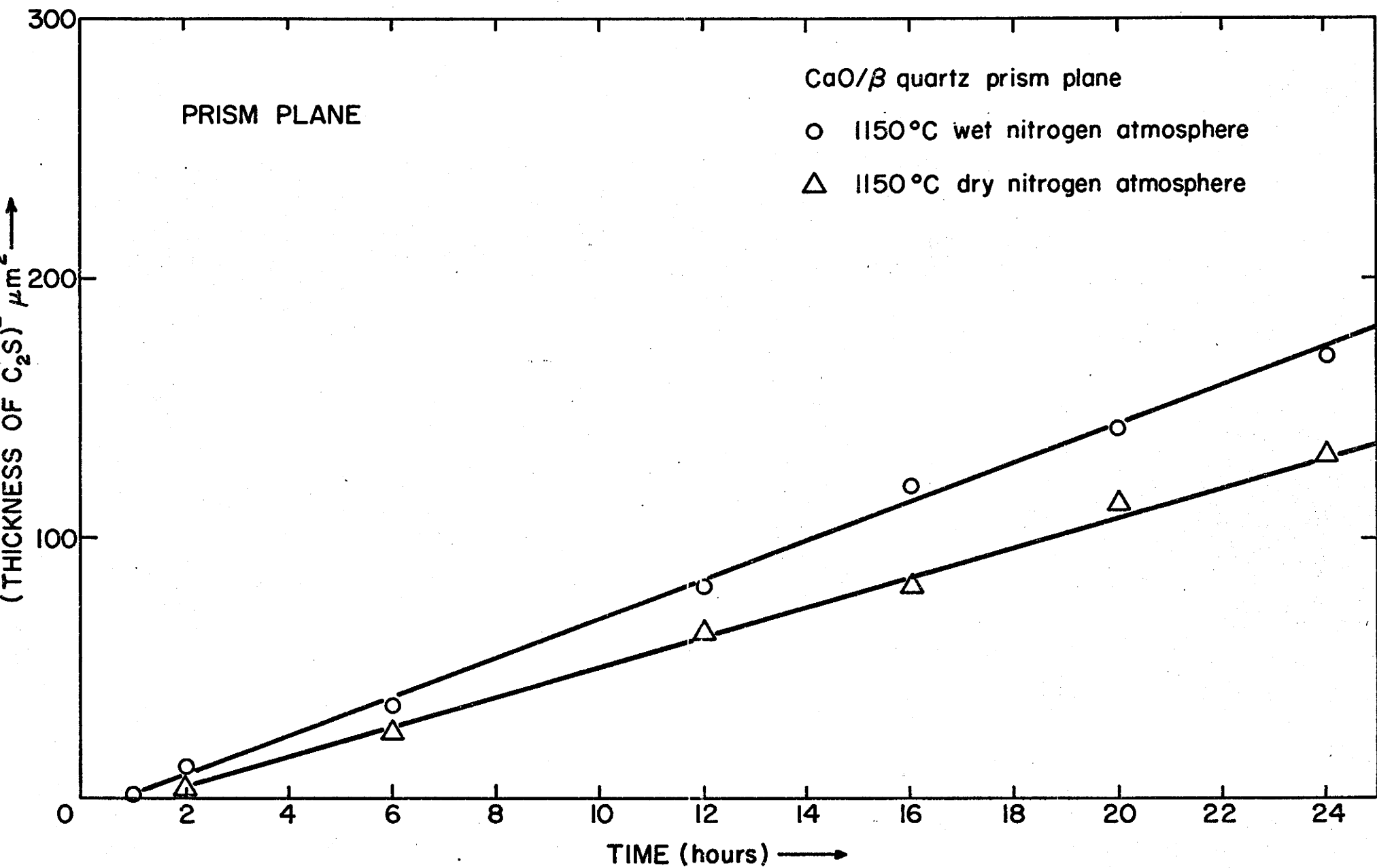
Figure III.6   Growth of C_2S on prism plane of β-quartz at 1100^OC
and 1050^OC in wet and dry nitrogen atmospheres.

CaO/β quartz, prism plane

△ 1100°C, wet N_2 atmosphere
○ 1100°C, dry N_2 atmosphere
▲ 1050°C, wet N_2 atmosphere
● 1050°C, dry N_2 atmosphere

PRISM PLANE

(THICKNESS OF $C_2S)^2$ μm^2

TIME (hours) ⟶

Figure III.7   Anisotropic growth of C_2S in wet and dry nitrogen
atmospheres at $1200^{O}C$.

CaO/β quartz prism plane

and CaO/β quartz basal plane   (1200 °C.)

○ wet N_2 atmosphere, basal plane

△ wet N_2 atmosphere, prism plane

▲ dry N_2 atmosphere, basal plane

● dry N_2 atmosphere, prism plane

BASAL AND PRISM PLANE

(THICKNESS OF C_2S)^2 μm^2

TIME (hours)
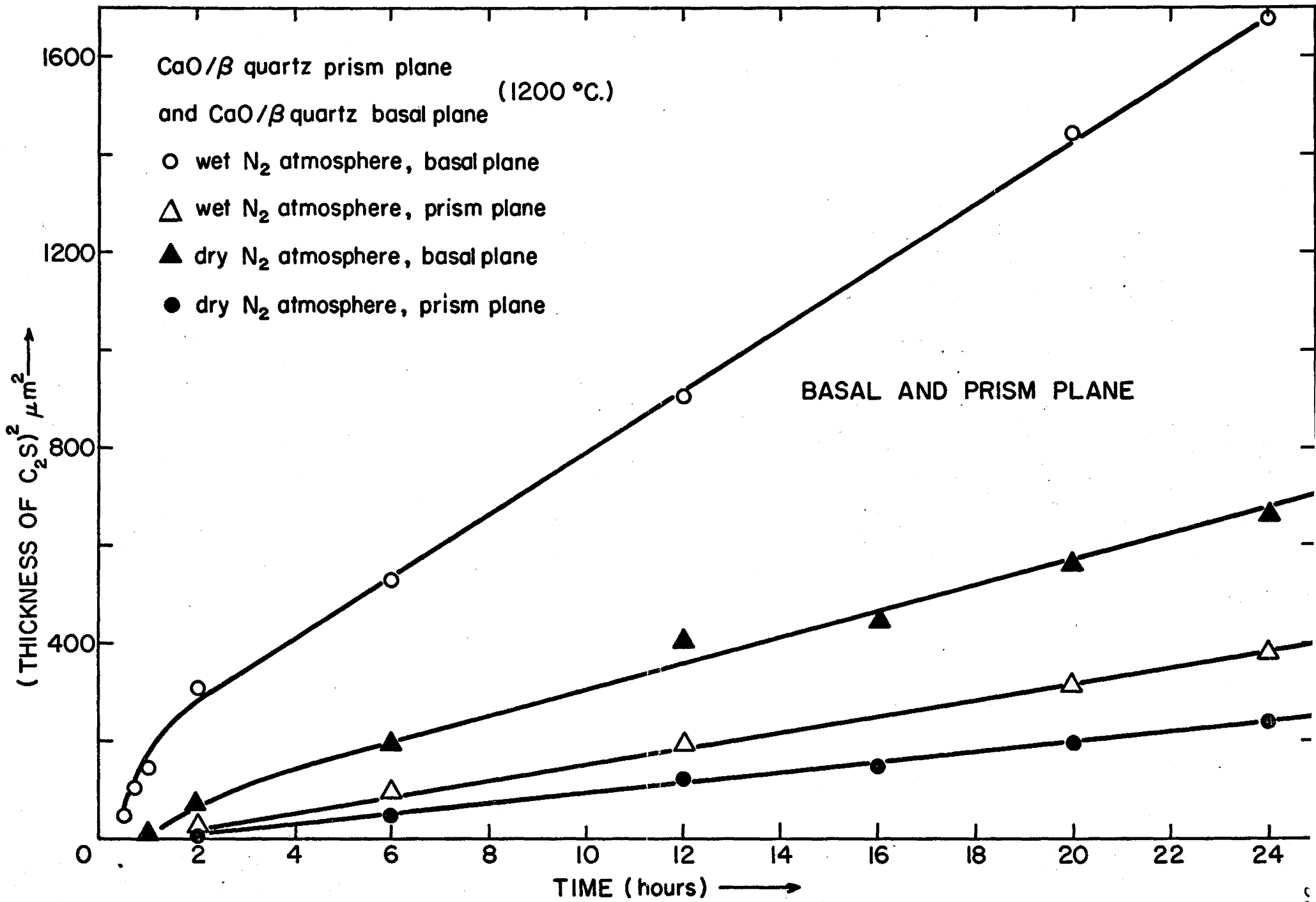
Figure III.8   Anisotropic growth of C_2S in wet and dry nitrogen

atmospheres at $1150^\circ C$.

CaO/β quartz basal plane and CaO/β quartz prism plane

1150 °C.

△ Basal plane, wet N$_2$ atmosphere
▲ Prism plane, wet N$_2$ atmosphere
○ Basal plane, dry N$_2$ atmosphere
● Prism plane, dry N$_2$ atmosphere

BASAL AND PRISM PLANE

(THICKNESS OF C$_2$S)^2 μm^2

TIME (hours)
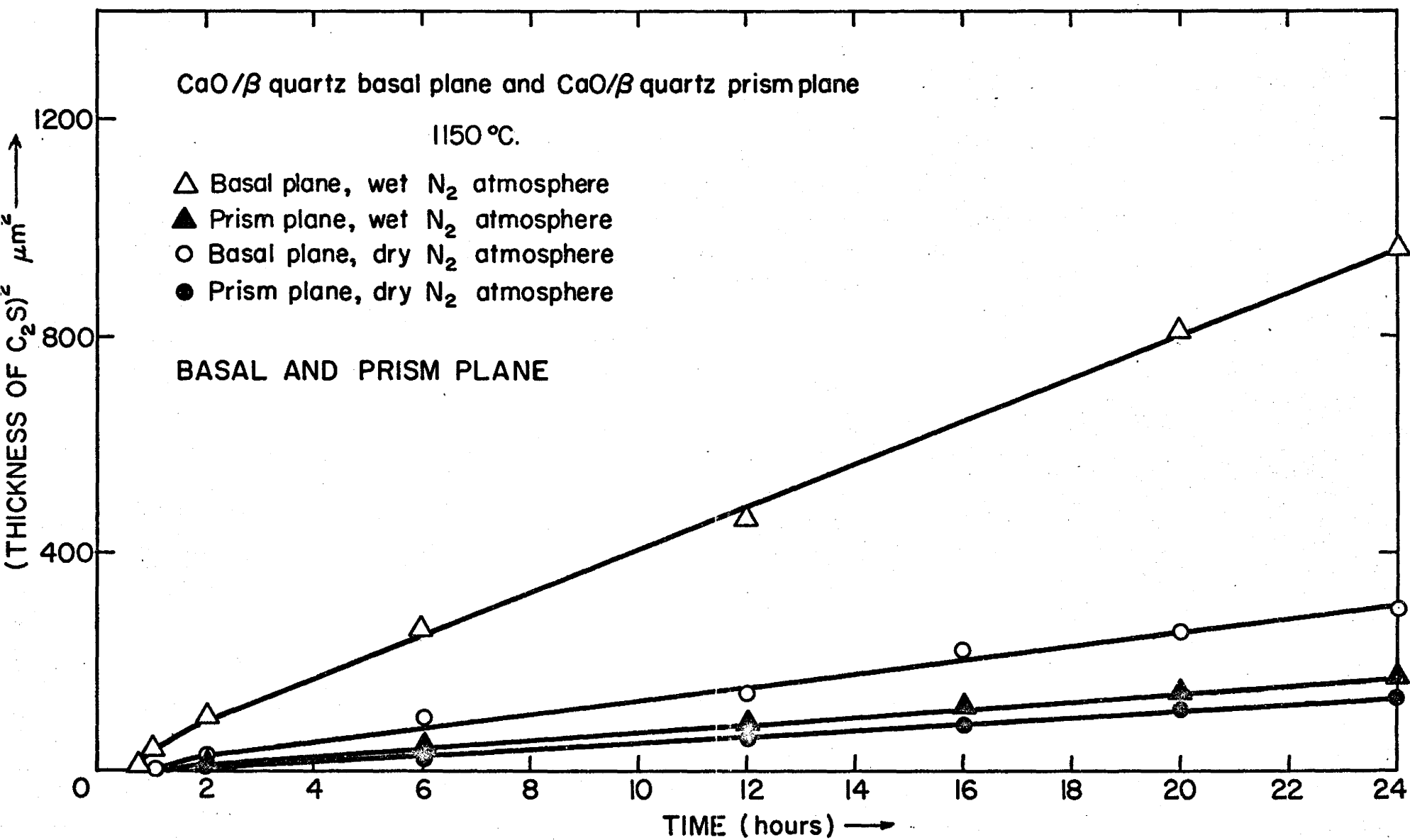
It is interesting to note that water vapor has an unequal enhancement effect on the reaction kinetics for the two crystallographic planes of β-quartz studied. The water vapor seems to bring about earlier nucleation of the first silicate layer on both the crystallographic planes. Figures III.1 and III.2 show a greater difference in the slopes of (thickness)^2 vs time plots in wet and dry atmospheres for basal plane than the corresponding difference for prism plane. Table III.1 summarises the results. At all the temperatures considered and under all atmospheres, the silicate layer was always found to nucleate first on the basal plane of the β-quartz.

The kinetic data also reveals the anisotropic nature of the product layer formation as shown in Figures III.8 and III.7. For any temperature in the range 1000°C to 1200°C, the CaO/SiO$_2$ reaction is faster on the basal plane of β-quartz than on the prism plane under both wet and dry nitrogen conditions. After 24 hours of reaction at 1200°C, a product layer of about 25 μm formed on the basal plane in dry nitrogen compared with 14 μm on the prism plane.

The definition of a rate constant k and an activation energy E for solid state reactions analogous to reactions taking place in gases or solutions gives rise to several difficulties for with a few notable exceptions, reaction rates increase rapidly with increasing temperature[46]. Furthermore, the temperature dependence of the rates of most reactions obeys an Arrhenius type equation (i.e., a linear relationship exists between the logarithm of the rate constant k and the reciprocal of the absolute temperature). In these circumstances it is always possible to define an empirical activation energy, E_A and frequency factor, A_A, by the equation:

$$k = A_A \, e^{-E_A/kT} \tag{1}$$

TABLE III.1

CaO/β-Quartz Reaction

Time of Reaction	Thickness of Product (C$_2$S) in μm on Basal Plane		Thickness of Product (C$_2$S) in μm on Prism Plane	
	Wet	Dry	Wet	Dry
1 hour	.12	2	2.0	< 1
2 hours	17.6	8	5	3
6 hours	23	14	10	7

In the reactions in gases or solutions, the rate constant is the proportionality factor between the reaction velocity and the concentration of the starting products. Thus it can be defined as the velocity for unit concentration. The dimensions of k are sec^{-1} for first order and $mol^{-1}sec^{-1}$ for second order reactions. The activation energy is derived from the dependence on temperature of k according to the Arrhenius law.

In solid state reactions, the concepts of concentration and order of reaction generally have no significance. The reaction velocity is defined as the change with time of:

i)   the thickness of the layer of product formed

ii) or of the weight of the layer

iii) or of the number of gram equivalents of product formed.

A rate constant cannot be defined in the same way as the reactions in gases or solutions. If we assume the same condition as for gas reactions, k must be independent of time and have the factor sec^{-1} in its dimensional formula, and increase with temperature according to an exponential law from which activation energy for reaction could be derived.

Tarnishing reactions, substitution reactions or double decomposition reactions follow the parabolic reaction rate law. As pointed out, the solid state reaction between CaO and SiO_2 in the temperature range 1000 - 1200°C appears to obey the parabolic reaction rate law in both wet and dry nitrogen atmospheres. In this case, the reaction velocity is governed by a diffusion process through a growing layer of product. The velocity of growth of the product is proportional to the reciprocal of x, the thickness

of the layer, hence $dx/dt = k_1/x$ which leads to $x^2 = 2k_1t$. The rate

constant, k_1, is expressed in cm^2/sec.

The slope of the plot of square of product layer thickness against

time is proportional to the parabolic reaction rate constant. The

logarithm of the slope (k) of the square of the thickness vs time plots

for the β-quartz/CaO reaction is plotted against a thousand times the

reciprocal of the absolute temperature (1000/T) in wet and dry atmospheres

for both planes considered in Figure III.9. The least square plots

indicate that the rate constant is exponentially related to the reaction

temperature. The linear relationship is observed in both wet and dry

atmospheres and on both planes. The slopes of the straight lines in the

dry and wet cases are the same, indicating that the activation energy for

the reaction is not influenced by the presence of moisture in the atmosphere.

The activation energy for the basal plane reaction was calculated to be

53 kcal/mole. This is in good agreement with the activation energy for

Ca^{+2} diffusion in well-crystallised α-dicalcium silicate (55 kcal/mole)

as reported by Lindner[47]. The prism plane activation energy was calculated

to be 63 kcal/mole and this is in good agreement with the value for

Ca^{+2} diffusion in α'-C_2S (65 kcal/mole) as reported by Lindner[47].

The intercepts on the log k axes under wet and dry conditions for

both planar directions considered are different, indicating a greater

pre-exponential factor (frequency factor) in the wet atmospheric conditions.

Assuming that the diffusion of Ca^{+2} through the C_2S product is the rate

controlling mechanism, it appears that there are more jump sites available

for Ca^{+2} diffusion in the product layer under wet atmospheric conditions.

The pre-exponential factor (A) values for all cases considered are tabulated

Figure III.9 Log k as a function of 1000/T where k is the slope of (thickness of $C_2S)^2$ vs t (time) plots and T is the absolute temperature of reaction.
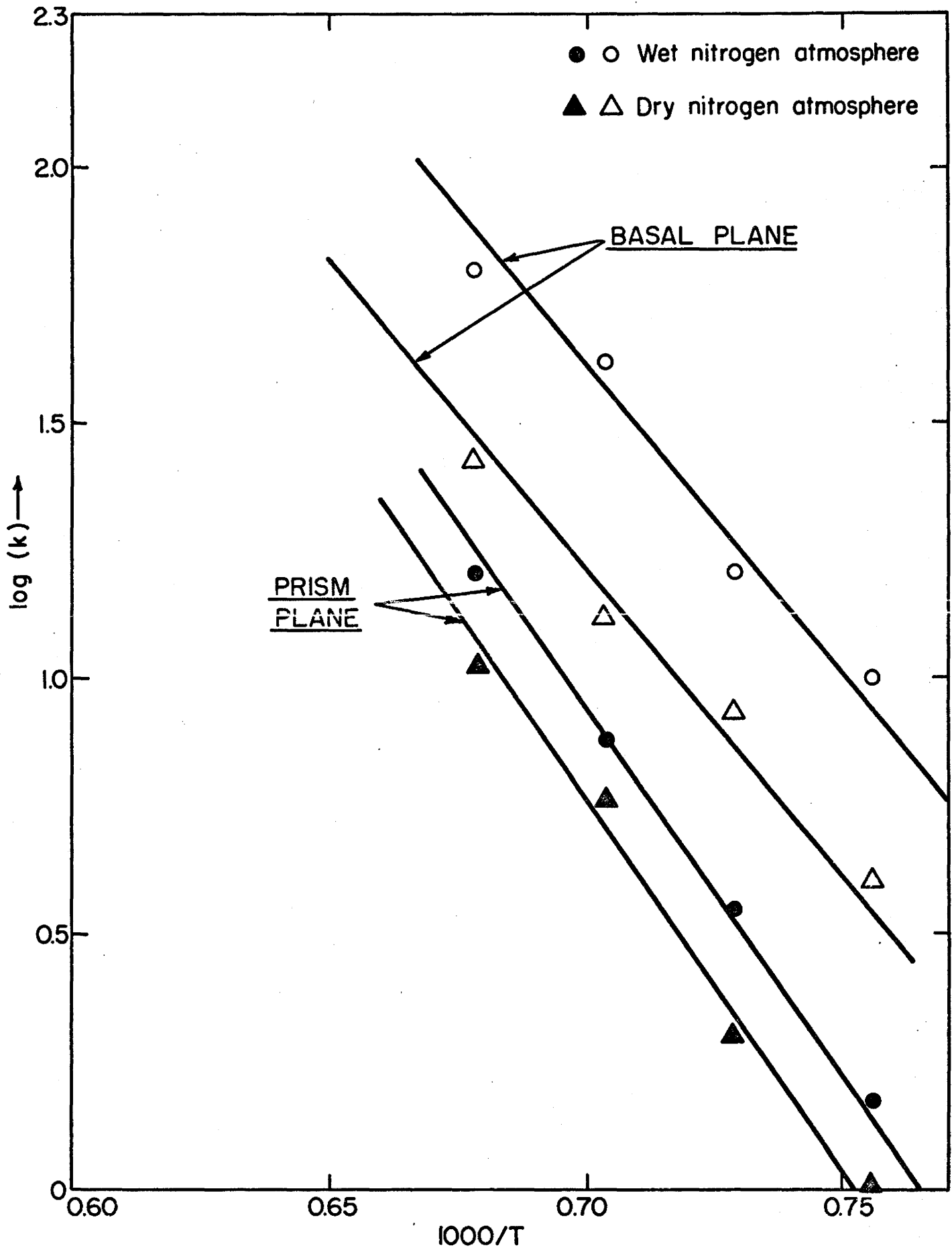
in Table III.2.

In summary, therefore, the observed parabolic reaction and the activation energies obtained for both crystallographic directions define Ca^{+2} as the possible rate controlling diffusing species. As the activation energy value is independent of the atmospheric conditions, the observed enhancement in the presence of water vapor is associated in some way with the availability of Ca^{+2} diffusion sites. The activation energy values of 53 kcal/mole and 63 kcal/mole on the basal and prism planes respectively indicate that α-C_2S product forms on the basal planes of the β-quartz and α'-C_2S on prism planes in the CaO/β-quartz reaction. The relative water enhancement in the two C_2S cases indicate that the α' product is less sensitive to the water vapor presence.

B. Reaction Mechanisms

Considering the solid state reaction $2AO + BO_2 \rightarrow A_2BO_4$ between two hypothetical oxides, if the reaction is diffusion controlled, the rate of thickening of product layer, $d(\Delta x)/dt$, will be inversely proportional to thickness, Δx, i.e.,

$$\frac{d(\Delta x)}{dt} = \frac{k}{\Delta x} \tag{2}$$

On integration, the result is the parabolic rate constant for the formation of the product layer. The different mechanisms by which such a reaction

TABLE III.2

INTERCEPTS ON LOG K AXIS IN FIGURE III.9

Plane	Wet Atmosphere (in μm^2/hour)	Dry Atmosphere (in μm^2/hour)
Basal	102.7	106.75
Prism	102.51	101.66

can proceed are illustrated in Figure III.10.

Mechanism (a) represents the diffusion of divalent cations and anions through the product layer giving the reaction at the product-BO_2 interface. If this mechanism occurs, markers placed at the original AO-BO_2 interface will be finally located at the AO-product interface. It is evident that this mechanism is independent of the oxygen activity in the surrounding gas atmosphere.

It is possible that anion diffusion through the product layer is slow with reference to cation diffusion and mechanisms such as "b" have been developed in which the oxygen follows the short circuit path through the gas phase whilst the divalent cations and the electrons diffuse through the product layer. The reaction sequence in this case is as follows:

i)   dissociation A^{+2} and O^{2-} in AO,

ii) reaction of O^{2-} anions to form oxygen gas at the specimen surface and excess electrons in the AO,

iii) simultaneous transport of oxygen through the gas phase and A^{2+} and the excess electrons with BO_2 to form A_2BO_4.

Mechanisms c and d are similar to a and b except that instead of A^{+2}, B^{+4} moves. Mechanism e considers concurrent cation diffusion of A^{+2} and B^{+4}. Mechanisms c and d will leave the markers at the BO_2 product boundary whereas mechanism e will leave them at the centre of the product A_2BO_4.

Marker experiments were conducted in the CaO-β quartz reaction to determine:

Figure III.10   Mechanisms of the reaction $2AO + BO_2 \rightarrow A_2BO_4$

(a)

AO | A_2BO_4 | BO_2

$A^{2+} \rightarrow$

$O^{2-} \rightarrow$

$2AO \rightarrow 2A^{+2} + 2O^{2-}$

$2A^{+2} + 2O^{2-} + BO_2 \rightarrow A_2BO_4$

(b)

$\uparrow O_2$ $\downarrow O_2$

AO | A_2BO_4 | BO_2

$2A^{2+} \rightarrow$

$4e^- \rightarrow$

$2AO \rightarrow 2A^{+2} + 2O^{-2}$

$2O^{2-} \rightarrow O_2 + 4e^-$

$O_2 + 4e^- \rightarrow 2O^{2-}$

$BO_2 + 2A^{+2} + 2O^{2-} \rightarrow A_2BO_4$

(c)

AO | A_2BO_4 | BO_2

$\leftarrow B^{+4}$

$\leftarrow 2O^{2-}$

$2AO + B^{+4} + 2O^{2-} \rightarrow A_2BO_4$

$BO_2 \rightarrow B^{+4} + 2O^{2-}$

(d)

$\downarrow O_2$ $\uparrow O_2$

AO | A_2BO_4 | BO_2

$\leftarrow B^{+4}$

$\leftarrow 4e^-$

$O_2 + 4e^- \rightarrow 2O^{2-}$

$2AO + B^{+4} + 2O^{2-} \rightarrow A_2BO_4$

$BO_2 \rightarrow B^{+4} + 2O^{2-}$

$2O^{2-} \rightarrow O_2 + 4e^-$

(e)

AO | A_2BO_4 | BO_2

$2A^{2+} \rightarrow$

$\leftarrow B^{+4}$

$2AO \rightarrow 2A^{2+} + 2O^{2-}$

$B^{+4} + 2O^{2-}$

$2AO \rightarrow A_2BO_4$

$BO_2 \rightarrow B^{+4} + 2O^{2-}$

$2A^{2+} + 2O^{2-} + BO_2 \rightarrow A_2BO_4$
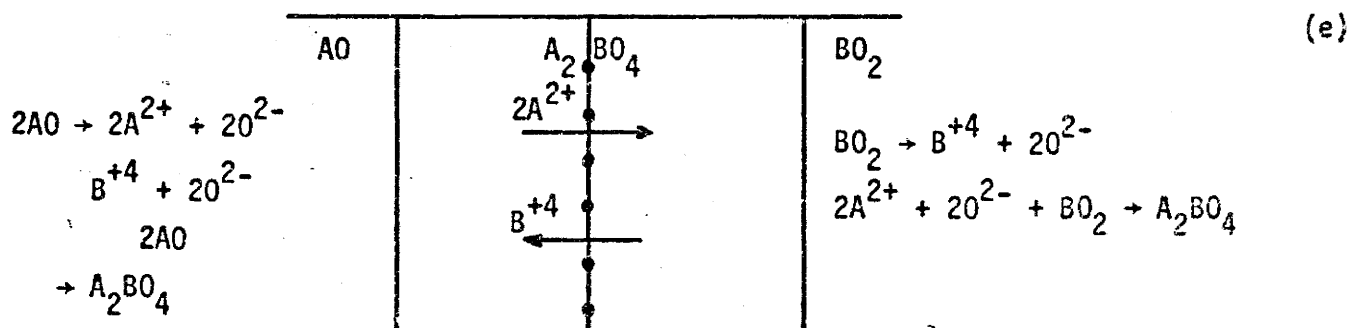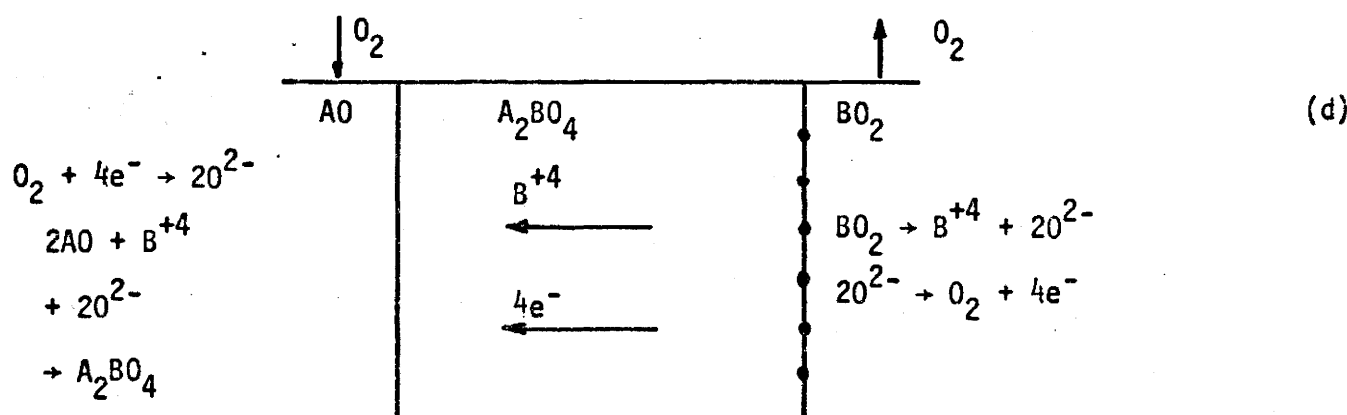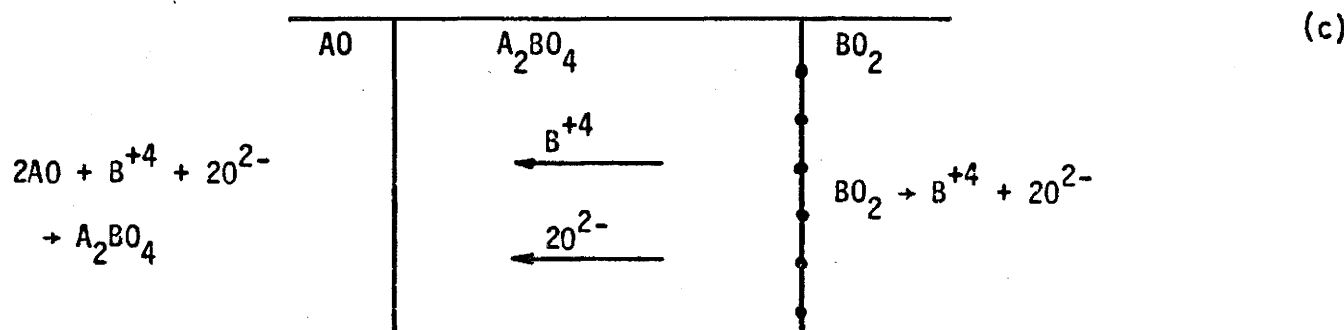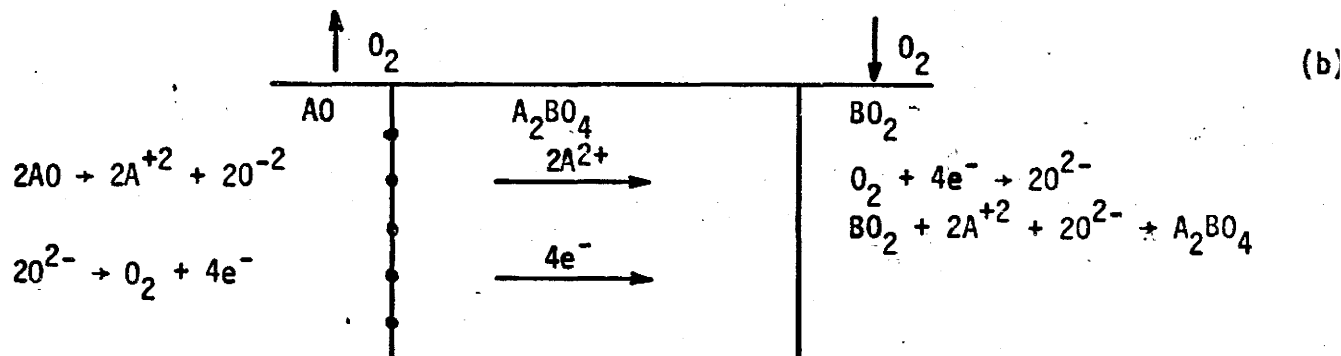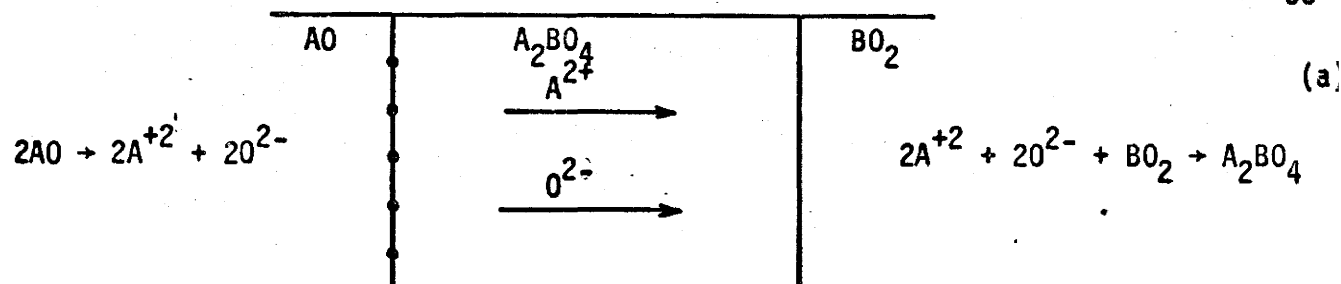
i) whether the reaction mechanism is the same in wet and dry atmospheres,

ii) whether the mechanism is the same for the reaction on the basal and prism planes of quartz.

The final marker position in the cases of CaO/basal plane β-quartz and CaO/prism plane of β-quartz, both in wet and dry atmospheres in the temperature range considered, was always found to be at the CaO/dicalciumsilicate boundary (Figure III.11). Figure III.12(a) indicates the marker position after the reaction on the basal plane at $1150^{\circ}C$ for 24 hours in wet nitrogen atmosphere and Figure III.12(b) indicates the same for the reaction on the prism plane at $1200^{\circ}C$ for 24 hours in dry nitrogen atmosphere. The same marker positions were noted in the dry/basal plane and wet/prism plane cases.

It may, therefore, be concluded that in both wet and dry atmospheres, the reaction between CaO and β-quartz is probably controlled by the diffusion of Ca^{+2} irrespective of the crystallographic direction of the β-quartz.

A definite mechanism by which water vapor creates more jump sites for diffusion in the silicate layer might become evident with further investigation. However, possible mechanisms will now be discussed. It is pertinent to note at this point that the degree of reaction enhancement under wet conditions increases with increasing temperature as shown in Figure III.13. This indicates that water vapor adsorption on the C_2S layer plays no controlling role in the reaction kinetics as the temperature dependence of adsorption is usually negative.

It is assumed in the following mechanisms that diffusion of Ca^{+2} species in the C_2S product is rate controlling. This assumption is based on
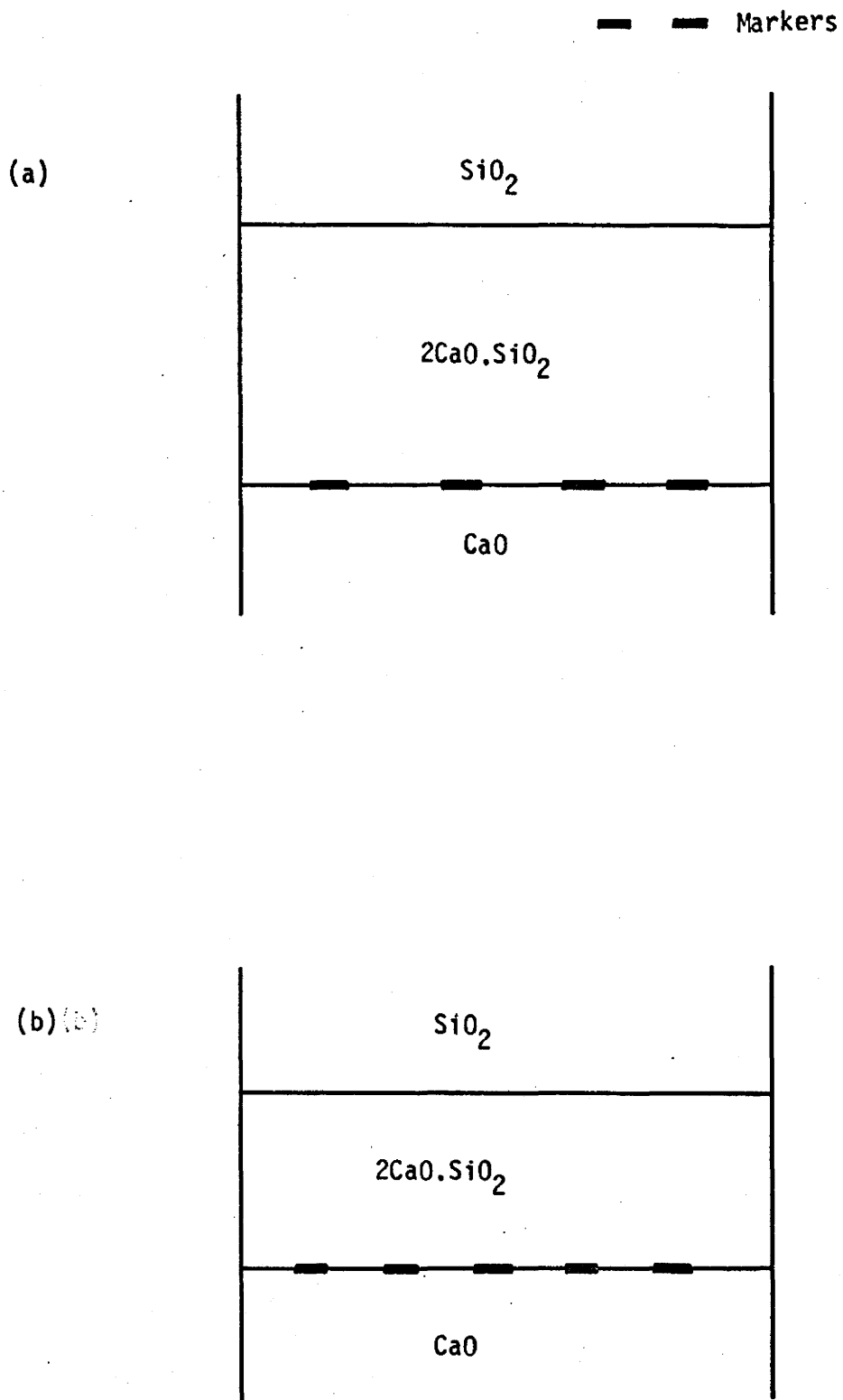
Figure III.11 (a) Marker position in wet atmosphere reaction.
           (b) Marker position in dry atmosphere reaction.

Figure III.12: Marker positions after the CaO-β quartz solid state

reaction on:

A. the basal plane at $1150^{O}C$ for 24 hours in wet N_2

atmosphere (x 480),

B. the prism plane at $1200^{O}C$ for 24 hours in dry N_2

atmosphere (x 352).

The bright spots at the dicalcium silicate product

layer - CaO boundary are the platinum markers. The

phase sequence is the same as in Figure III.11.
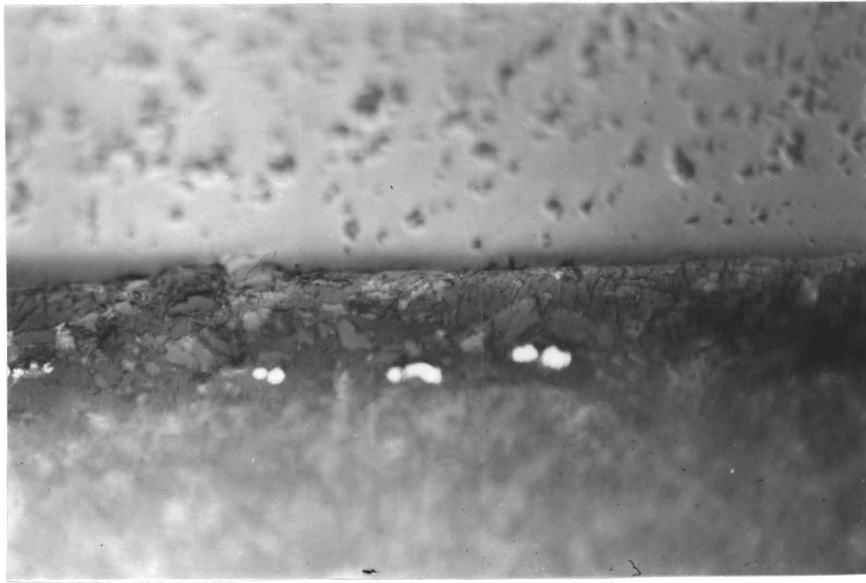
A

B

Figure III.13   Growth of C_2S on basal plane in wet
N_2 atmosphere at $1200^{\circ}C$, $1150^{\circ}C$,
$1100^{\circ}C$ and $1050^{\circ}C$.

CaO/β quartz basal plane in
wet N₂ atmosphere

○ — 1200 °C.
△ — 1150 °C.
▲ — 1100 °C.
● — 1050 °C.
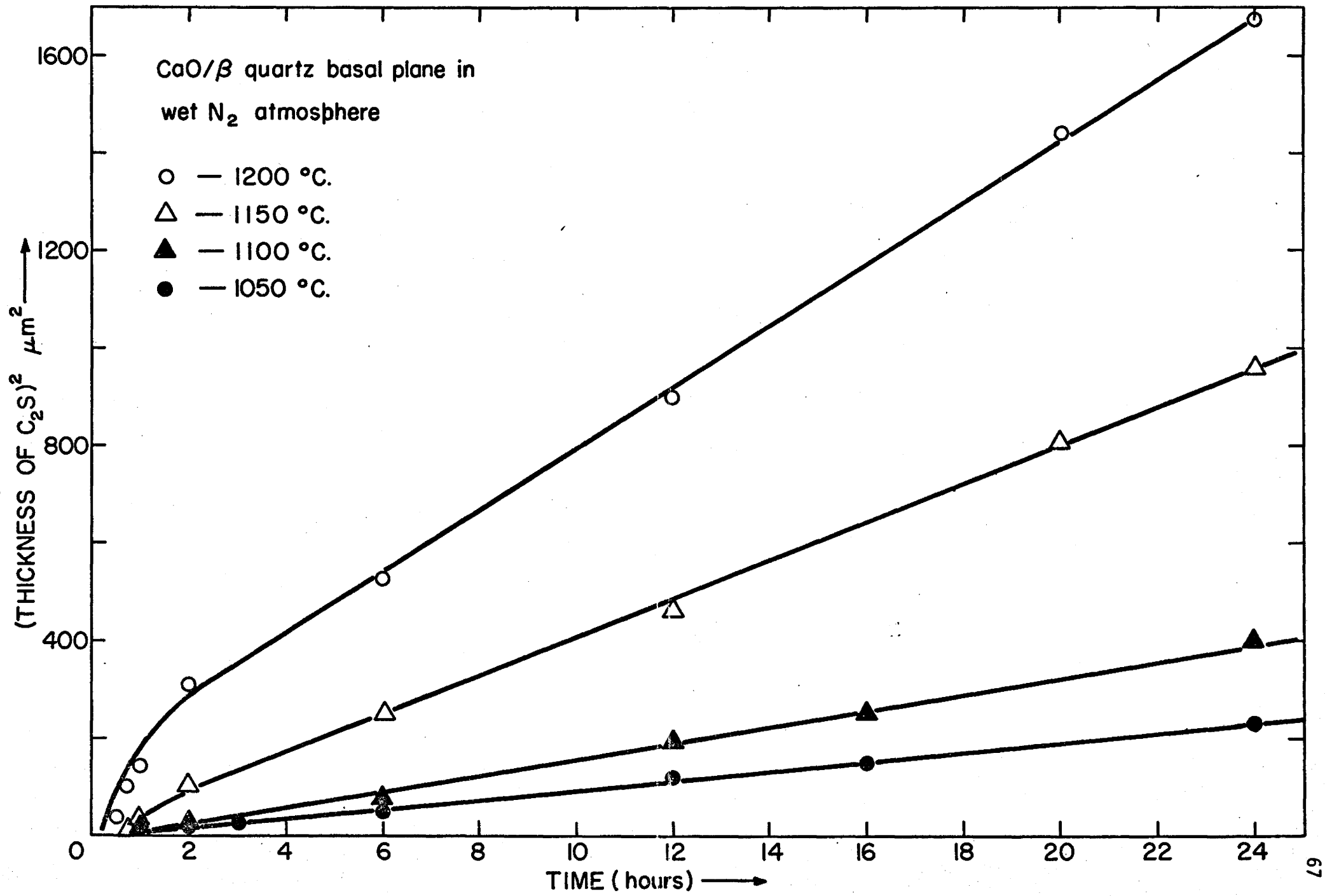
the present activation energy results and the frequent observation of cation diffusion control in diffusion phenomena such as sintering and high temperature creep in ceramic systems. Coble[48] explains the anomalous control in terms of anion grain boundary diffusion and small fissures in the product C_2S could also contribute. The following reaction could occur:

$$(\equiv Si - O - Si \equiv)_L + H_2O \rightarrow (\equiv Si - OH \uparrow OH - Si \equiv)_L \qquad (3)$$
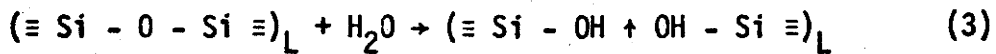
where L represents the lattice of dicalcium silicate and $\uparrow$ represents the breakage of $\equiv Si - O - Si \equiv$ bridge following the creation of two hydroxyl (silanol) sites -- a process which "loosens" the C_2S lattice and creates openings through which interstitial diffusion of Ca^{+2} could occur. This reaction could also be expressed as follows:

$$H_2O + O_L^{2-} + CaO + O^{2-} \square \; '' + 2e \rightleftharpoons Ca_i^{+2} + O_L^{2-} + 2(OH^-)_L \qquad (4)$$
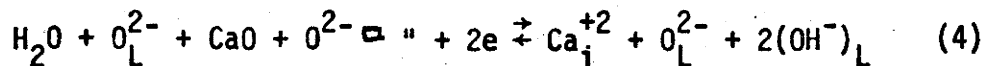
where L represents the lattice of Ca_2SiO_4, $O^{2-}\square$ an anion vacancy, e excess electrons and Ca_i^{+2} a calcium cation in interstitial site.

There is strong evidence of SiO_3OH groups in hydrated dicalcium silicate at lower temperatures[23]. Even though such hydroxyl groups are expected to be unstable in silicates at 1000 - 1200°C, they might be capable of metastable existence in small concentrations at such high temperatures.

The incorporation of $2(OH^-)$ into the lattice however involes the decomposition of the water molecules.

The combination of two hydroxyl groups to give a water molecule is very important in dehydration of clays and hence it has been a subject of great interest to ceramists. In dehydration reactions, in order to form one

H_2O molecule from two OH^- groups, the proton of one of

the OH^- groups must in some way become mobile. Because of the large rates

of dehydration reaction observed, it appears that the actual concentration

of such mobile protons is much larger than expected by assuming that the

proton diffuses through the solid in a classical sense. To explain the

higher proton mobility, the concept of "proton tunnelling"[49] was

suggested. Hydrogen bonding is thought, in essence, to be a tunnelling

phenomenon in which the probability of finding the proton is distributed

over two locations separated by an energy barrier. The necessary

condition for tunnelling is that on both sides of the separating

barrier corresponding energy levels are available, one of which is empty.

Since classical diffusion jumps using highly excited levels can occur

only at temperatures like 5000^OK the only possibility left is the transfer

of the proton from one OH^- group to a neighbouring OH^- group by non-classical

tunnelling either on the lowest energy level, n_o, or on the first excited

level.

On the basis of tunnelling[50] mechanism, Freund has indicated the

possible equilibrium reactions as:

$$O^{2-} + HOH \rightleftarrows OH^- + OH^- \qquad (5)$$
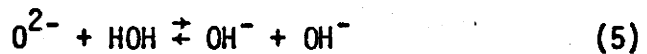
In the case of C_2S and water vapor reaction the "dehydration" reaction is

possibly "reversed" and the L→R reaction of (5) occurs. The oxygen anion in

equation (5) in this case belongs to the C_2S lattice.

The other way of increasing the Ca^{+2} diffusion sites in C_2S would

be to create Ca^{+2} vacancies ($Ca^{+2}\square$) in the C_2S lattice as a result of

its reaction with moisture in the atmosphere. Both CaO and SiO_2 are metal excess (n type) semiconductors. In the present investigation, the production of C_2S (dicalcium silicate) as a result of CaO/β-quartz reaction was carried out always in the presence of excess CaO. Therefore the reaction of water with C_2S to produce $Ca^{2+}\square$ in the C_2S lattice seems unlikely.

In the present investigation, the two polymorphs of C_2S, i.e., α C_2S (monoclinic or hexagonal) and α' C_2S (orthorhombic) show different degrees of sensitivities to the presence of moisture. This is consistent with the well known fact that the reactivity of different polymorphs of C_2S towards water is different[23].

In the light of previous work on H_2O/SiO_2 reaction, it is suggested that enhanced interstitial diffusion of Ca^{+2} probably occurs in the presence of water vapor.

C. Diffusional Anisotropy in β-Quartz

The anisotropic nature of Ca^{+2} diffusion in β-quartz is demonstrated by the concentration profiles of calcium in the <0001> and the <10$\bar{1}$0> directions at 1200°C in wet atmospheres as shown in Figure III.14(a),(b) (region A).

Frischat[17] investigated the temperature dependence of the diffusion coefficient of Ca^{+2} parallel to the c axis of quartz and found it to obey the expression $D = 10^5 \exp(-68kcal/RT)$ between 600 and 820°C.

Figure III.14   Distribution of Ca and Si in the cross section of
                 a sample in a) <0001> and b)<1010> directions of
                 β-quartz.
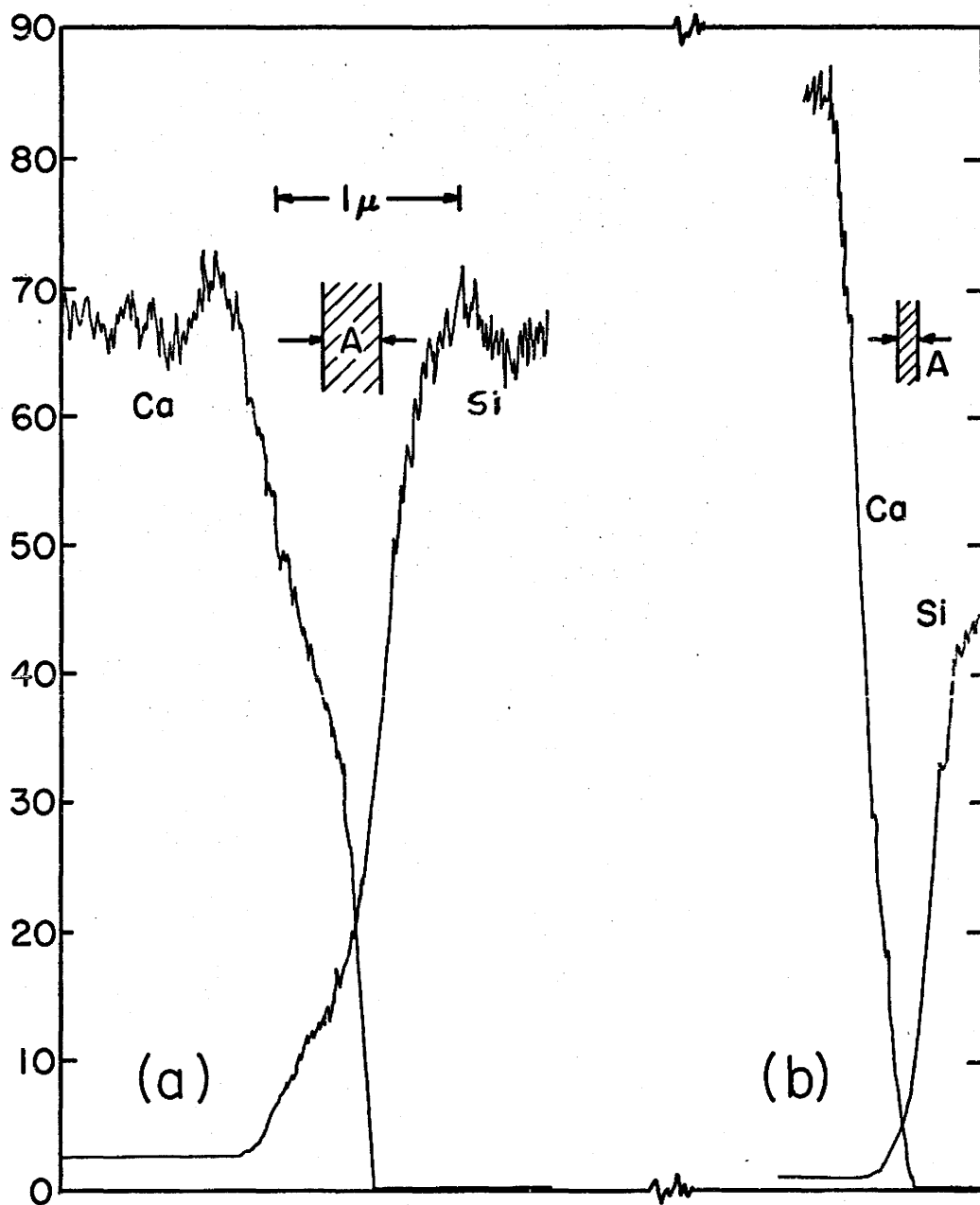
a) count rate on Ca standard 1000 cps
   count rate on Si standard 1000 cps

b) count rate on Ca standard 1000 cps
   count rate on Si standard 2000 cps

D. Effect of Water Vapor on Calcium Diffusion in β-Quartz

The effect of water vapor on CaO/SiO_2 solid state reaction is two-fold:

i)   it enhances the calcium diffusion in the silica and hence produces early nucleation of the silicate layer, and

ii) once the first silicate layer forms, the water vapor continues to enhance the growth of the silicate layer. This particular aspect of the effect of water vapor has already been considered in Section A of this chapter.

Young[18] indicated that water vapor physically adsorbs on the silanol (hydroxyl) sites of the silica surface. Drury, Roberts and Roberts[19] presented a mechanism of water diffusion in silica glass. They suggested that water vapor breaks Si-O bridges, so widening the holes present in the lattice and allowing calcium to diffuse more easily. On comparison of the calcium and silicon concentration profiles obtained for samples reacted at $1200°C$ for 24 hours in wet nitrogen atmospheres and dry nitrogen atmospheres, it was found that there is deeper calcium penetration into the quartz under wet conditions, as demonstrated in Figure III.15(a) and (b) (region A). It can be also noticed that the dicalcium silicate layer in the wet atmosphere sample is thicker than that in dry atmosphere samples.

Figure III.15 Distribution of Ca and Si across the
cross section of sample in
a) wet and
b) dry nitrogen atmospheres.
Region A in a and b shows greater Ca
penetration in β-quartz in wet con-
ditions than in dry conditions.

Count rate on Ca standard 2000 cps
Count rate on Si standard 1000 cps
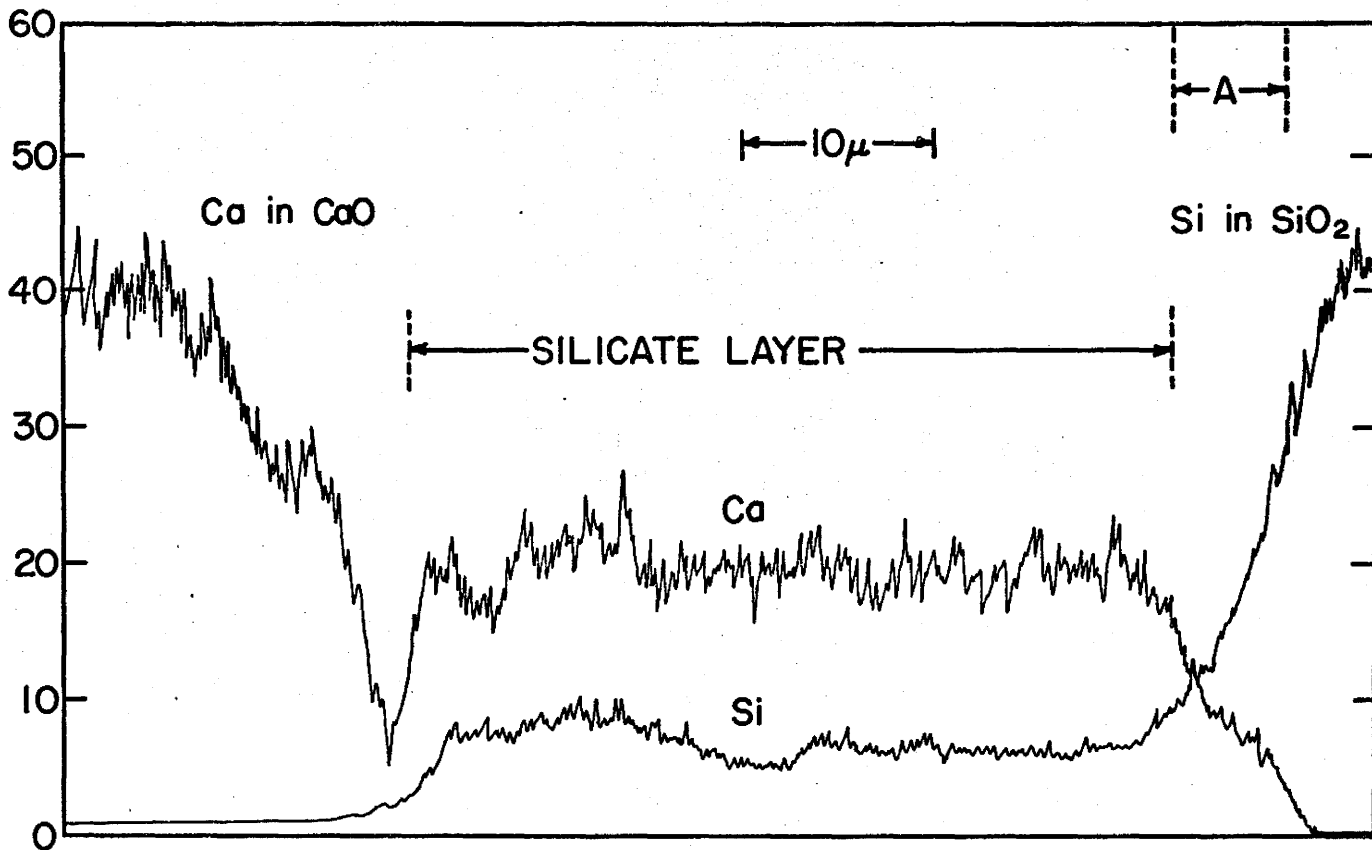
(a)

(b)
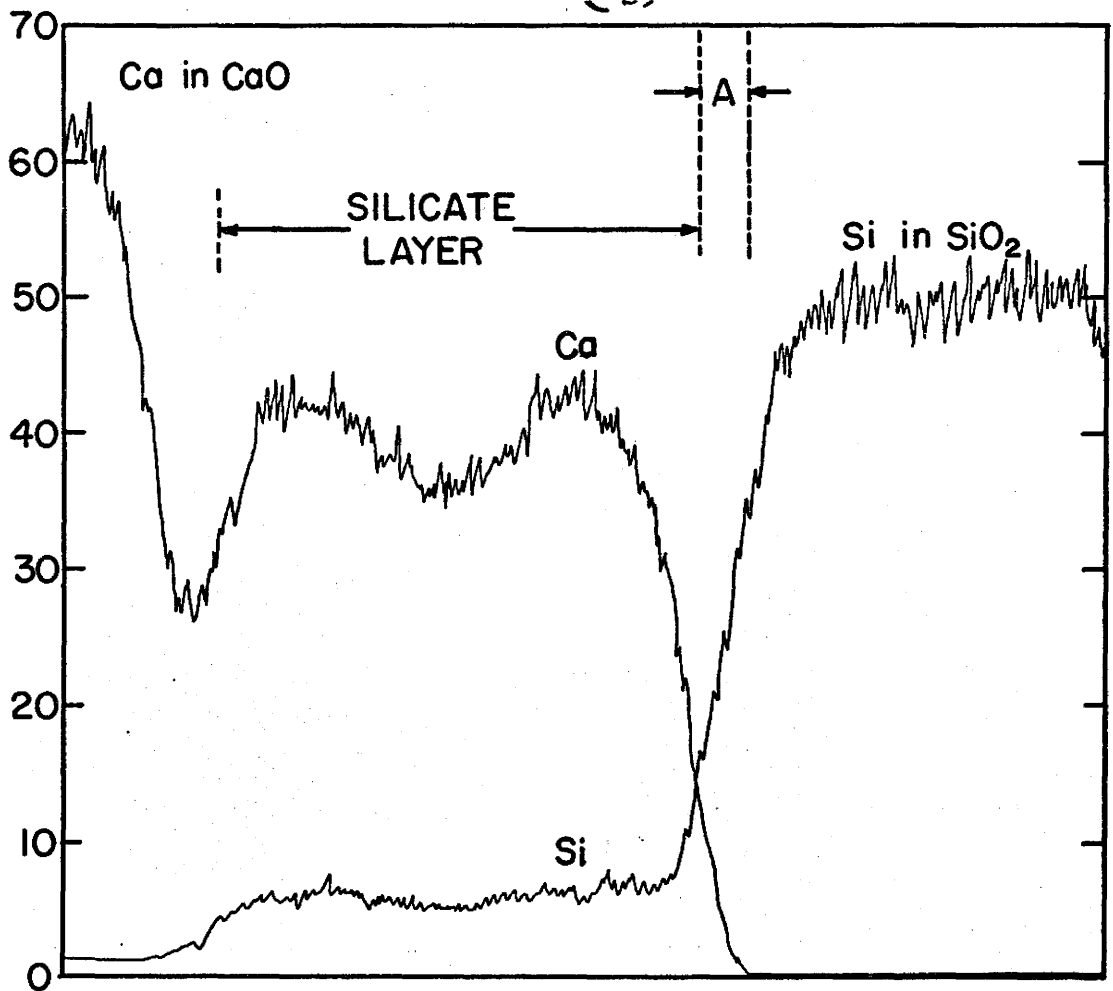
E. Nucleation of Dicalcium Silicate in the CaO/β-Quartz Reaction

Some indication as to how the first dicalcium silicate layer
nucleates can be obtained from the concentration profiles of calcium in
the initial stage of the reaction. Concentration profiles of calcium in
the <0001> direction of β-quartz single crystals at $1100^{\circ}C$ reacted in
wet nitrogen atmosphere after 15, 30, 45 and 60 minutes of reaction are
shown in Figure III.16. Concentration profiles after 15 minutes of
reaction (Figure III.16(a)) appears to indicate a little migration of Ca^{+2}
into the β-quartz structure. Figure III.16(b) indicates that after 30 minutes of
reaction there is a little more calcium penetration into the β-quartz.
But still there is no reaction layer of definite composition. Figure III.16(c)
indicates that more calcium has diffused into the quartz structure after
45 minutes of reaction and the system is tending to form a silicate layer.
Figure III.16(d) shows that a silicate layer is formed after 60 minutes of
reaction. The same kind of concentration profiles were obtained for the
sample reacted in dry atmospheres.

It appears that there is a penetration of Ca^{+2} into the β-quartz
structure and it increases very slowly with increasing time of reaction.
As previously indicated water vapor is thought to break some of the Si-O
bonds that surround the interstices in the crystal making it easier for
Ca^{2+} to diffuse. As more calcium enters the quartz lattice, the lattice
could become strained. Some evidence of such "strain" was obtained by Taylor[20]
in that quartz X-ray lattice parameter changes were noted as a result of
Ca^{2+} diffusion. As a possible result of this solid solution of the calcium,
higher concentrations of Ca^{+2} build up in the surface regions of the β-quartz.
The existence of such strains in the surface of the β-quartz could

Figure III.16   Distribution of Ca and Si in <0001> direction of
β-quartz across the cross section of sample
reacted at 1100°C in wet N_2 atmosphere after
a) 15 minutes
b) 30 minutes
c) 45 minutes
d) 60 minutes
of CaO/β-quartz reaction.

Counts on Ca standard in all → 1000 cps
Counts on Si standard   a) 1000 cps
                        b) 2000 cps
                        c) 1000 cps
                        d) 2000 cps
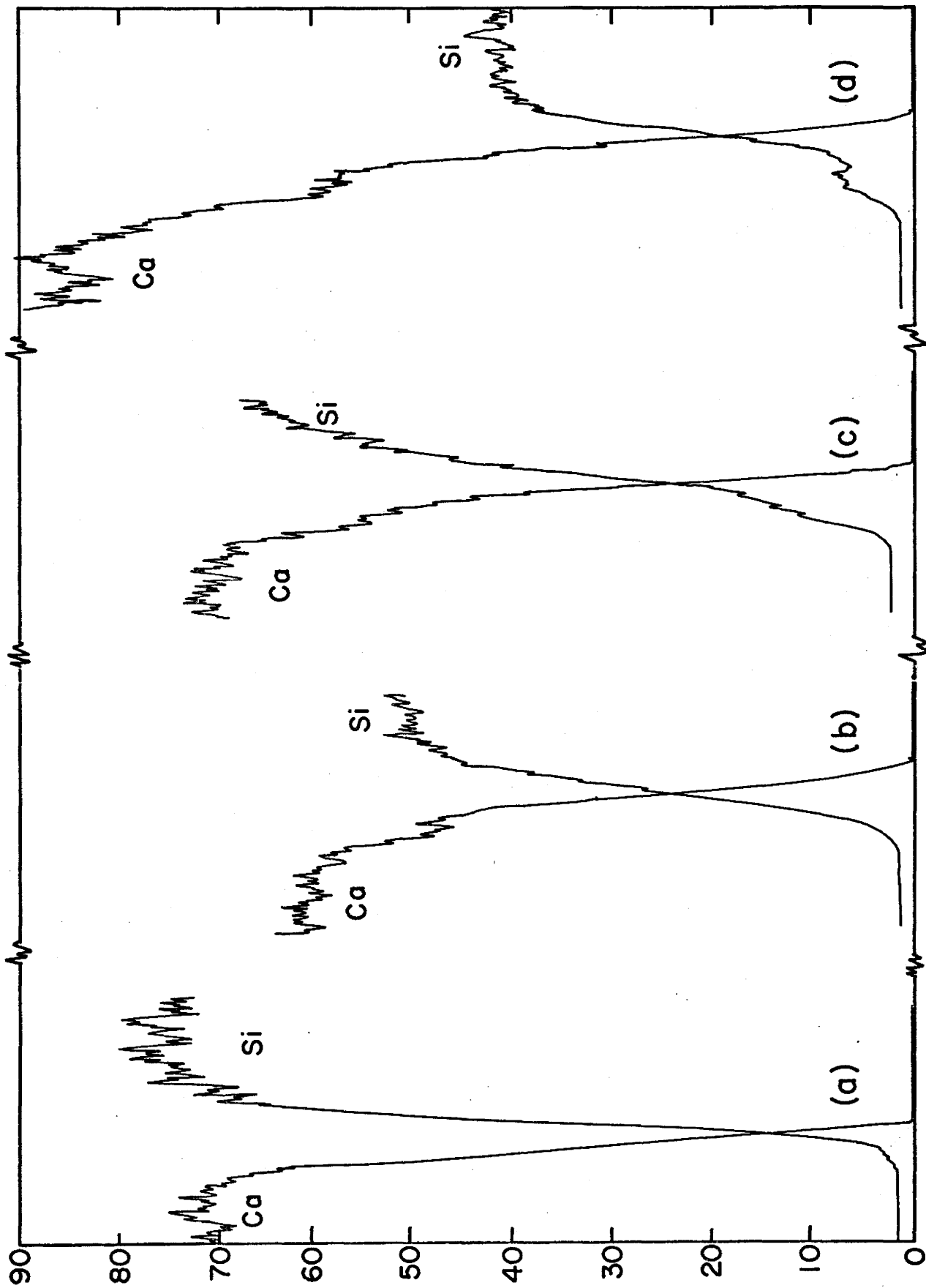
be the reason for the colour changes observed in geological thin section analysis by transmitted plane polarised light. A color micrograph of a thin section of the sample reacted at 1150°C for 24 hours in a wet nitrogen atmosphere is shown in Figure III.17. The product layer is orange/red, the β-quartz appears light green to yellow and the dark blue peripheral layer might correspond to a region of strain. This colour change might possibly be due to a variation in thickness of the β-quartz piece as a result of the thinning process. But this seems unlikely because of the presence of hard epoxy in the sample. Also, if there is a thickness variation in the β-quartz due to the thinning process, the surface of the quartz would likely be convex-upward. If that were so, the bire-fringent colour observed should go from first order yellow (centre) to a first order white. In fact, the opposite sequence is observed and the order of colour from the centre cut, increases. Therefore the peripheral colour of the β-quartz is probably not due to any thickness variations. A strained high calcia region in the β-quartz surface could play a key role in the nucleation of the calcuium orthosilicate layer.

The process of nucleation of calcium orthosilicate from this strained region may be analogous to the process of age hardening in the aluminum-copper system. In that system the first step in the precipitation from the supersaturated solid solution is the segregation of copper atoms into clusters or platelets a few angstroms thick and approximately 100 $\overset{o}{A}$ diameter but still part of the parent lattice. These platelets are called Guinier Preston zones or G.P.1 zones. In the next step, copper atoms diffuse to the G.P.1 zones to form a larger or G.P.2 zone (θ"), 8 $\overset{o}{A}$ thick and 150 $\overset{o}{A}$ diameter. This θ" precipitate maintains fit or coherency by distorting aluminum planes and thus gives rise to a coherency strain. These strain fields which
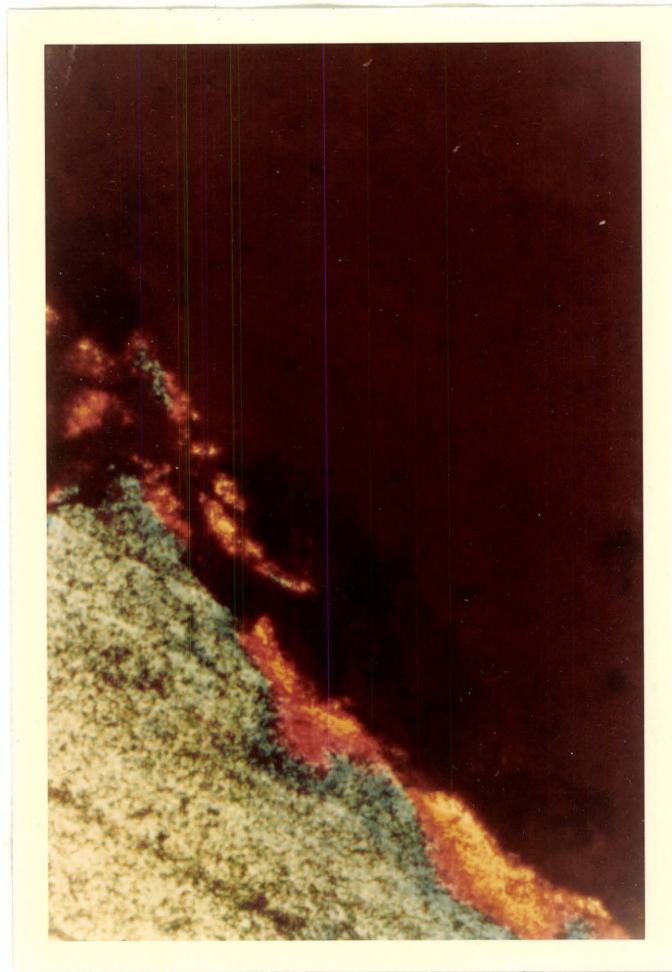
Figure III.17   A colour micrograph in transmitted plane polarised light
of the thin section of sample reacted at $1150^{\circ}C$ for 24
hours in wet conditions.

The orange/red colour might correspond to the product
layer. The light green/yellow colour corresponds to quartz.
The dark blue peripheral colour might correspond to a
region of strain in quartz.

have a much larger effective size than the precipitate, oppose the movement of dislocations, i.e., harden the alloy. At a still later stage, a new transition phase, θ'', still partially coherent with the matrix, is precipitated and produces maximum hardness.

Nearly all the age hardening systems show an ageing sequence.

zones → intermediate precipitates

→ equilibrium precipitates

The intermediate precipitate may be partially coherent or completely coherent.

In the CaO/β quartz reaction the sequence could be as follows: - when calcium diffuses in silica through the channels in the lattice, it endeavors to maintain coherency with the lattice and therefore no silicate forms. The concentration profiles of Ca and Si in the sample heated for 45 minutes (Figure III.16(c)) show that although there is no silicate layer of definite composition, there is some sort of rearrangement of calcium and silicon atoms. This may be comparable to the intermediate precipitate in age hardenable alloys and seems to be partially coherent. Heating for one hour results in the formation of a precipitate which has an entirely different crystal structure, and a definite composition. This precipitate is incoherent. The kinetics of the growth of this silicate layer has already been discussed in detail. Before the silicate layer attains a definite thickness, its growth is non-parabolic and the reaction may be interface controlled. The diffusion of species in the thin layer of silicate is definitely not the rate controlling step. But once the

silicate layer is sufficiently thick, the diffusion of species in the layer becomes the rate controlling step. The further growth of the silicate layer then obeys the parabolic rate law both in wet and dry atmospheres.

CHAPTER IV

CONCLUSIONS

i) The solid state reaction between CaO and β-quartz at tempera-
tures in the range between $1000^{o}C$ and $1200^{o}C$ is anisotropic in
both wet and dry nitrogen atmospheres, and is enhanced in the
presence of moisture. It appears that α-C_2S forms on the basal
and α' -C_2S on the prism planes of the quartz.

ii) The extent of water vapor enhancement is a function of crystallo-
graphic planes of β-quartz on which the reaction takes place.

iii) The presence of moisture produces more enhancement in the
kinetics of reaction on the basal plane than on the prism plane
of β-quartz. This is possibly due to the fact that different
polymorphs of C_2S (α and α'-dicalcium silicate) with different
sensitivities to the presence of moisture are produced on
different crystallographic planes of β-quartz.

REFERENCES

1. Blanks, R.F., and Kennedy, H.L., "The Technology of Cement and Concrete", Vol. 1, 27-35, John Wiley and Sons Inc., New York, 1955.

2. Rankin, G.A., and Wright, F.E., "Ternary System $CaO-Al_2O_3-SiO_2$", Am. J. Sc., Fourth Series, 39, 229, 1-79, 1915.

3. Swayze, M.A., "A Report on Studies of the Ternary System $CaO-C_5A_3-C_2F$ and the Quaternary System $CaO-C_5A_3-C_2F-C_2S$ as Modified by 5% Magnesia", Am. J. Sc., 244, 1, 65, 1946.

4. Eickel, E.C., "Cements, Limes and Plasters", 272-73, John Wiley and Sons, Inc., New York, 1928.

5. Witt, J.C., "Portland Cement Technology", 184, Chemical Publishing Company, Inc., New York, 1966.

6. Singer, F. and Singer, S.S., "Industrial Ceramics", 119-20, Chemical Publishing Company, Inc., New York, 1963.

7. Sosman, R.B., "The Phases of Silica", 34-263, Rutgers University Press, New Brunswick, 1964.

8. Eitel, W., "Silicate Science - III", 134-39, Academic Press, New York, 1965.

9. DeKeyser, von W.L., and Cypres, R., "The Mineralising Effect of Kaolin and Feldspar on the Transformation of Silica", Ber Deut Keram Ges, 38, H7, 303-08, 1961.

10. Verhoogen, J., "Ionic Diffusivity and Electrical Conductivity in Quartz", Am. Mineral, 37, 637-55, 1952.

11. Pfenninger, H., and Laves, F., "Cation Migration and Colour Centre Formation During Electrolysis of Quartz Plates Perpendicular to the Optical Axis", Naturwiss, 47, 276, 1960.

12. Rybach, L., and Laves, F., "Sodium Diffusion Experiments in Quartz Crystals", Geochim. Cosmochim. Acta, 31, 539-46, 1967.

13. White, S., "Ionic Diffusion in Quartz", Nature, 225, 375-76, 1970.

14. Mortley, W.S., "Diffusion Paths in Quartz", Nature, 221, 359, 1969.

15. Frischat, G.M., "Cation Transport in Quartz Crystals I - Sodium Diffusion Parallel to the c Axis", Ber Deut Keram Ges, 47, 4, 238-43, 1970.

16. Frischat, G.H., "Cation Transport in Quartz Crystals II - Sodium Diffusion Perpendicular to the c Axis", Ber Deut Keram Ges, 47, 5, 313-16, 1970.

17. Frischat, G.H., "Cation Transport in Quartz Crystals III - Calcium Diffusion Parallel to the c Axis, Ber Deut Keram Ges, 47, 6, 364-68, 1970.

18. Young, G.J., "Interaction of Water Vapor with Silica Surfaces", J. Coll. Sc., 13, 67-85, 1958.

19. Drury, T., Roberts, G.J., Roberts, J.P., "Diffusion of H_2O in Silica Glass", Advances in Glass Technology, Plenum Press, New York, 1962.

20. Taylor, D., "Calcium Solid Solution in Quartz in the Presence of Water Vapor, 35-42, Unpublished B.Sc. Thesis, University of Utah, 1967.

21. Eitel, W., "Silicate Science - I", 1-19, Academic Press, New York, 1964.

22. Ramberg, H., "Relative Stabilities of Some Simple Silicates as Related to the Polarisation of the Oxygen Ions", Am. Mineralogist, 39, 256-71, 1954.

23. Wells, A.F., "Structural Inorganic Chemistry", 787-802, Oxford University press, 1962.

24. Midgley, C.M., "The Crystal Structure of β-Dicalcium Silicate", Acta Cryst., 5, 307-12, 1952.

25. Bredig, M.A., "Polymorphism of Calcium Orthosilicates", J. Amer. Ceram. Soc., 33, 6, 188-92, 1950.

26. Lehmann, H., Niesel, K., Thormann, P., "Stability Fields of Polymorphic Forms of C_2S", Tonind Ztg. Keram. Rundsch, 93, 6, 197-209, 1969.

27. Schwiete, H.E., Kroenrt, W.K., and Deckert, K., "Existence of Ranges and Stabilisation of High Temperature Modifications of C_2S", Zem Kalk. Gips, 21, 9, 359-66, 1965.

28. Megaw, H.D., "The Structure of Afvillite $Ca_3(SiO_3OH)_2.2H_2O$", Acta Cryst., 5, 479-91, 1952.

29. Heller, L., "The Structure of Dicalcium Silicate α-Hydrate", Acta Cryst., 5, 724-28, 1952.

30. Taylor, H.F.W., "Aspects of Crystal Structures of Calcium Silicates and Aluminates", J. Appl. Chem. (London), 10, 8, 317-23, 1960.

31. Mamedov, K.S., and Belov, N.V., "Crystal Structures of Tobermorite", Doklady Akad. Nawk, SSSR, 123, PI, 163-65, 1958.

32. Megaw, H.D., and Kelsey, C.H., "Crystal Structure of Tobermorite", Nature, 177, 4504, 390-91, 1956.

33. Taylor, H.F.W., "Transformation of Tobermorite into Xonotlite", Mineral. Mag., 32, 245, 110-16, 1959.

34. Majdic, A., and Henning, H., "Diffusion of Calcium and Silicon in the Liquid Binary System CaO-SiO$_2$", Ber. Deut. Keram. Cres., 47, 1, 53-59, 1970.

35. Jander, W., and Hoffman, E., "Solid State Reactions at High Temperatures - The Reaction Between Calcium Oxide and Silicon Dioxide", Z. Anorg. Allg. Chem., 218, 211-23, 1934.

36. Steinour, H.H., "The System CaO-SiO$_2$-H$_2$O and the Hydration of the Calcium Silicates", Chem. Rev., 40, 3, 391-460, 1947.

37. Taylor, H.F.W., "Hydrated Calcium Silicates I", J. Chem. Soc., (London), 726, 3682-90, 1950.

38. Greenberg, S.A., "Reaction Between Silica and Calcium Hydroxide Solutions I J. Phys. Chem., 65, 1, 12-16, 1961.

39. Logginov, G.I., Rebinder, P.A., Abrasenkova, V.F., "Interaction of Calcium Hydroxide at Ordinary Temperatures with Sand of Different Densities", Colloid J. (English Translation) 21, 4, 429-34, 1959.

40. Moorehead, D.R. and McCartney, E.R., "Hydrothermal Formation of Calcium Silicate Hydrates", J. Am. Cer. Soc., 48, 11, 565-69, 1965.

41. Jander, W., "Solid State Reactions at High Temperatures", Z. Anorg. Allg. Chem., 163, 1-30, 1927.

42. Kakitani, S., and Fujisaka, M., "Solid State Reaction Between Calcium Carbonate and Silica", Yogoyo Kyokai Shi, 66, 133, 1958, abstracted in Ceramic Abstracts (6) 173b, 1959.

43. Verduch, A.G., "Initial Stages of the Reaction Between Cristobalite and Calcium Carbonate", Bull. Soc. Esp. Ceram., 3, 6, 594-602, 1964.

44. Benz, R., and Wagner, C., "Thermodynamics of the Solid System CaO-SiO$_2$ from Electromotive Force Data", J. Phys. Chem., 65, 1308-11, 1961.

45. Montierth, M.R., Gordon, R.S., and Cutler, I.B., "The Initial Stages of the Reaction between Quartz and Calcium Carbonate", Materials Science Research, Vol. 4, Plenum Press, New York, 522-44, 1969.

46. Gomes, W., "Definition of Rate Constant and Activation Energy in Solid State Reactions", Nature, 192, 4805, 865-66, 1961.

47. Lindner, R., "Studies on Solid State Reactions with Radiotracers", J. Chem. Phys., 23, 410, 1955.

48. Coble, R.L., "Model for Diffusion Controlled Creep in Polycrystalline Materials", J. Appl. Phys., 34, 1679, 1963.

49. Rouxhet, P.G., Touillaux, R., Mestdagh, M., and Fripiat, J.J., "New Considerations about the Dehydroxylation Processes of Minerals", Proceedings of the International Clay Conference, Vol. 1, Israel University Press, 109-19, 1969.

50. Freund, F., "Dehydroxylation Mechanism of Clay Minerals: The Initial Conversion of Hydroxyl Groups into Water Molecules by Proton Tunnelling", Proceedings of the International Clay Conference, Vol. 1, Israel University Press, 109-19, 1969.